



System reliability analysis of soldier-piled excavation in unsaturated soil by combining random finite element and sequential compounding methods

A. Johari¹ · A. R. Kalantari¹

Received: 20 May 2020 / Accepted: 22 October 2020 / Published online: 23 November 2020
© Springer-Verlag GmbH Germany, part of Springer Nature 2020

Abstract

The stability of excavation in unsaturated soil is closely related to the variation of soil properties and matric suction. Determination of different failure modes and identifying the contribution of each one in an unsaturated soldier-piled excavation are the vital aspects of system reliability analysis. To address these issues, this paper provided a stochastic framework with a random elasto-plastic finite element-based program coded in MATLAB to evaluate the reliability indices of individual failure modes with considering the inherent uncertainty of real site soil properties and unsaturated state. In the next step, the sequential compounding method (SCM) was utilized to obtain the system reliability index by compounding the reliability indices of individual failure modes. Numerical results of a case study showed that in all failure modes, considering unsaturated state not only increases the mean value of factor of safety (FS) but also decreases the related standard deviation, which can be counted as a goal of reliability analysis. Among the reliability indices of the components, the most critical one is attributed to the lateral displacement. Furthermore, the safety ratio concerning the shear force has the maximum reliability index compared to the others. Moreover, based on the coefficient of variation (COV) of the components, it was found that the uncertainty of the soil parameters has the most significant effect on the global safety factor of the excavation.

Keywords Random finite element method · Unsaturated soil · System reliability analysis · Soldier-piled excavation

Introduction

Soldier piles are widely used in urban and industrial areas as a temporary or permanent retaining system for constructing the underground structures. The major advantages of this retaining wall system are its relatively low cost and fast construction. For these reasons, the soldier piles are a popular topic and have attracted the attention of researchers (e.g., Zhang 2009). To evaluate the performance of soldier-piled excavation, considering not only multiple failure modes but also soil properties uncertainties and the unsaturated state are crucial.

However, some studies have been presented in the literature for stability analysis of retaining wall in the unsaturated state (e.g., Vo and Russell 2014), but there is still a need for

the implementation of this state in stability analysis of soldier-piled excavation. Sahoo and Ganesh (2018) investigated the distribution of active earth pressure against the face of retaining wall with unsaturated backfill. The results showed that the resultant active force exerted by unsaturated clay backfill was significantly affected by flow condition, while in the case of unsaturated sand backfill, active earth pressure remained unaffected. Shwan (2016) extended the limit analysis method to evaluate passive earth pressure in an unsaturated state. Vahedifard et al. (2015) developed a method for calculating earth pressures exerted by unsaturated backfill against retaining wall, which tackles the limitation connected with analytical methods in an unsaturated condition such as collapse and effective stress. Vo and Russell (2016) compared different retaining wall model tests with theoretical results in the unsaturated state.

Several studies showed the insufficiency of traditional deterministic excavation stability analysis in which stability is evaluated only based on the FS (e.g., Baecher and Christian 2005). Due to the inherent variability associated with soil properties and a limited number of boreholes, a reliability-

✉ A. Johari
johari@sutech.ac.ir

¹ Department of Civil and Environmental Engineering, Shiraz University of Technology, Shiraz, Iran

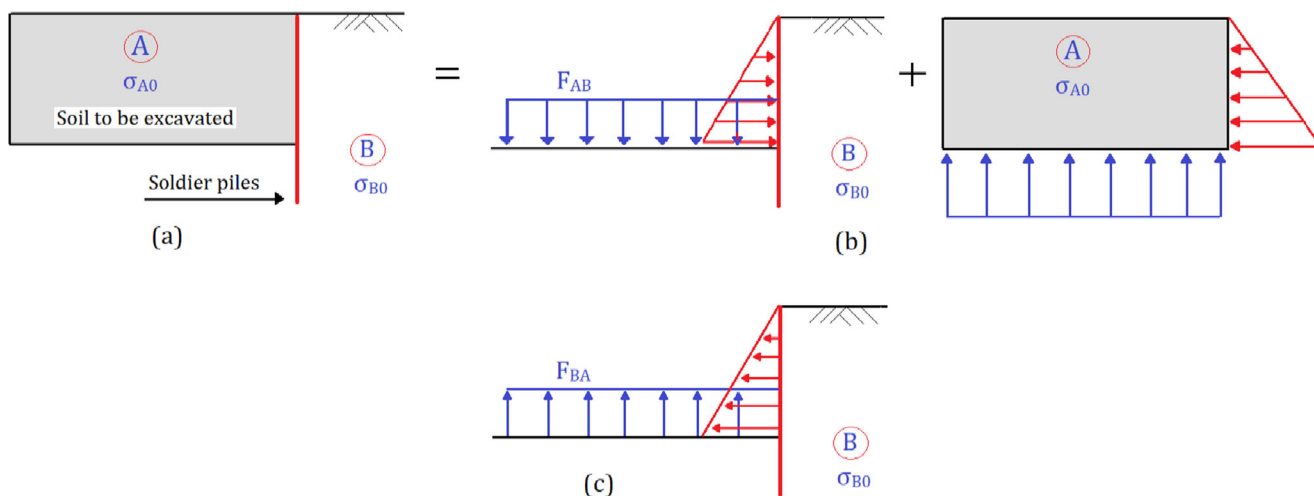


Fig. 1 The procedure for determining the excavation forces. (a) Initial stress state. (b) Equilibrium of the bodies (A and B). (c) Excavation forces F_{BA}

based approach is present as a complementary measure to the FS to aid geotechnical experts to make acceptable designs (Johari and Mousavi 2019; Parhizkar et al. 2012). The relevant studies have addressed the probabilistic evaluation of the retaining system (e.g., Gao et al. 2019), but none of these involved a soldier-piled excavation. Wang (2013) presented a Monte Carlo simulation (MCS)-based design of a retaining system and found that factors adopted in Eurocode 7 do not satisfy its goal reliability. GuhaRay and Baidya (2015) combined the probability of failure (P_f) and sensitivity of a random variable of sheet pile wall and introduced a new factor, namely probabilistic risk factor. Due to a disability of probabilistic method to consider the spatial variability of soil properties, in the early 1990s, Griffiths and Fenton (1993) proposed a new probabilistic analysis approach called the random finite element method (RFEM). This method has been used for various geotechnical problems, but few studies involved the stability of excavation. Tang (2011) evaluated the excavation-induced lateral deflection and presented a design chart for estimating the P_f with respect to lateral deflection. Sert et al. (2016) assessed the role of spatial variability of sand properties on lateral displacement and bending moment of retaining wall using RFEM. Luo et al. (2018) conducted a probabilistic analysis of supported excavations using RFEM

and revealed that spatial variation of soil properties has an essential role in several responses such as displacement and internal forces of the wall.

Most reliability analysis mainly focuses on the reliability index (β) corresponding to an individual failure mode, while geotechnical problems often involve numerous failure modes. As noted in the work of Luo et al. (2018), the failure modes to be considered in the design of a soldier-piled excavation may include global stability, lateral displacement, shear force, and bending moment. Since the system reliability index of soldier-piled excavation can be less than the reliability index of the individual failure mode, it is essential to use a system reliability analysis (Liu and Low 2017). System reliability analysis of the retaining system is rarely found in the literature. However, system reliability analysis of other geotechnical problems such as slope stability has received a great deal of attention recently (e.g., Johari and Lari 2017; Metya et al. 2017). Zevgolis and Daffas (2018) developed a model to investigate the system reliability of the soil nail wall. Zevgolis and Bourdeau (2010) conducted a system reliability analysis of retaining wall considering external stability as a series system. The result of this research indicated that the degree of correlation has an important effect on the overall P_f . Luo and Das

Table 1 Theoretical autocorrelation functions used to determine the autocorrelation lengths

Model no.	ACF function	Autocorrelation lengths
1	$\rho_{\Delta z} = \begin{cases} 1 - \frac{ \Delta z }{a} & \text{for } \Delta z \leq a \\ 0 & \text{for } \Delta z \geq a \end{cases}$	a
2	$\rho_{\Delta z} = e^{-(\Delta z /b)}$	$2b$
3	$\rho_{\Delta z} = e^{-(\Delta z /c)^2}$	$\sqrt{\pi c}$
4	$\rho_{\Delta z} = e^{-(\Delta z /d)} \left(1 + \frac{ \Delta z }{d} \right)$	$4d$

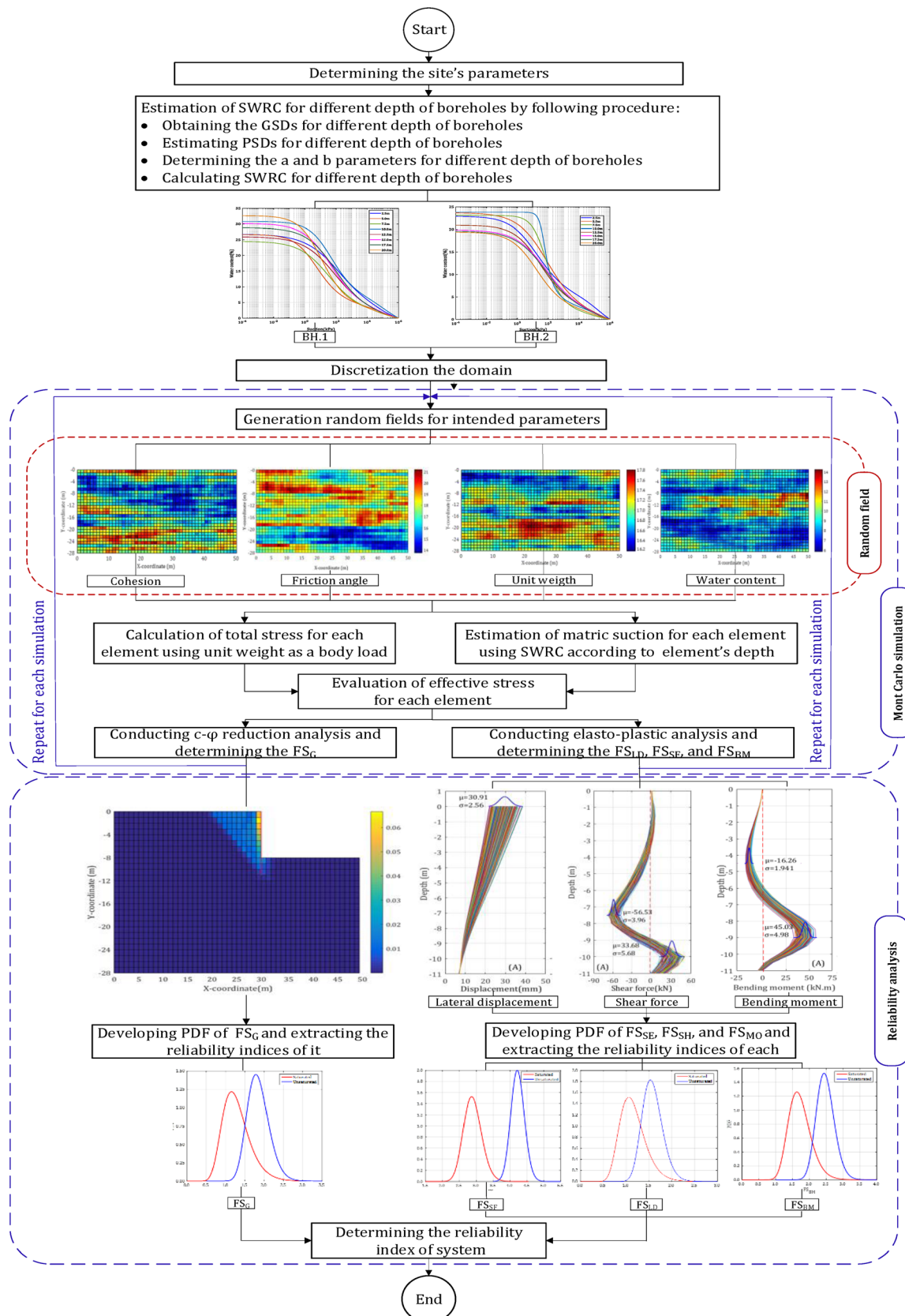


Fig. 2 Flowchart of system reliability analysis of soldier-piled excavation in an unsaturated state

(2016) evaluated the system reliability of serviceability, including excessive wall deflection and excessive ground surface settlement, for braced excavations, which cause damage to adjacent infrastructures.

The common feature of the mentioned stochastic studies was the consideration of spatial variability of soil properties in the retaining systems without considering unsaturated state, all geotechnical and structural failure modes, two-dimensional random field, and system reliability analysis. The main aim of the current study was to cover the mentioned limitations via system reliability analysis of unsaturated soldier-piled excavation using RFEM. To do this, a real soldier-piled excavation in the unsaturated state was analyzed deterministically using finite element-based program coded in MATLAB. Then, reliability analysis was performed using RFEM by the implementation of the random field in the program that was mentioned earlier to consider the inherent uncertainty of soil properties (i.e., cohesion, friction angle, and unit weight). Moreover, the effect of the unsaturated state was evaluated by using a physico-empirical model and considering water content (ω_c) as a random variable. Then, the reliability indices of all individual failure modes (i.e., global, lateral displacement, shear force, and bending moment) were estimated. Finally, system reliability analysis was performed to offer a single index for quantifying the overall reliability of the system, instead of several partial reliabilities indices.

Methodology of analysis

In the present study, stochastic stability analysis of soldier-piled excavation in the unsaturated state is assessed. For this purpose, the random field is utilized in conjunction with the finite element method (FEM) to study the spatial variability of regionalized variables. In this way, the soil is assumed to be unsaturated, and the multiple failure modes of soldier-piled excavation are considered. Brief descriptions of the selected methodology are presented in the following subsections.

Finite element modeling

FEM is a powerful tool to model geotechnical problems such as excavation. One of the superiority of this method is the ability to predict the deformations of soldier-piled excavation. In the excavation project, the soil is removed from the ground. Since the ground is stressed before the removal of its part, the analysis must simulate the correct stress for remaining soil by applying force along the excavation surface, as shown in Fig. 1. Generally, the excavation forces (F_{BA}) acting on a boundary depending on the stress state in the excavated soil (σ_{A0}) and the self-weight of it, regardless of the retaining system (Smith et al. 2013). Forces F_{BA} can be calculated as follows:

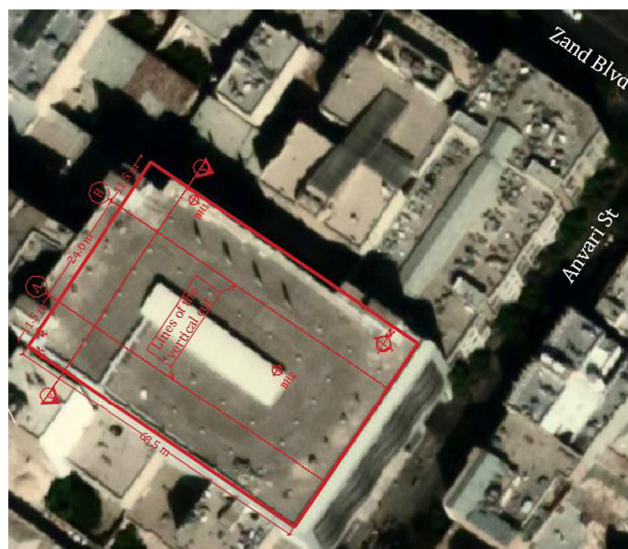


Fig. 3 Satellite overview of site location

$$\{F_{BA}\} = \int_{V_A} [B]^T \{\sigma_{A0}\} dV_A + \gamma \int_{V_A} [N]^T dV_A \quad (1)$$

where $[B]$ is the strain-displacement matrix, V_A the excavated volume, γ the soil unit weight, and $[N]$ the shape functions of elements.

Failure limit states of soldier-piled excavation

Generally, for designing soldier-piled excavation, three main limit states: external stability, serviceability, and structural must be considered (Luo et al. 2018). Each of these limit states includes several failure modes with varying degrees of importance due to location, neighboring structures, and the depth of excavation. In order to demonstrate these limit states, the FS was used in relevant equations in this section for all the failure modes.

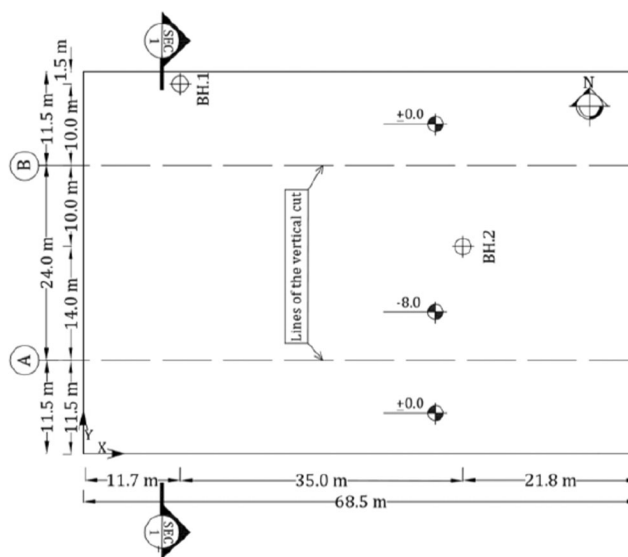


Fig. 4 Relative location of the boreholes

Table 2 Geotechnical soil properties from BH.1

Depth (m)	Classification	LL (%)	PI (%)	γ_{mean} (kN/m ³)	ω_c (%)	SPT	Friction angle (Deg.)	Cohesion (kN/m ²)
2.5	CL	26.23	7.44	16.58	6.99	25	15.33	20.62
5.0	ML	23.26	3.50	16.87	7.38	26	16.17	21.27
7.5	CL-ML	26.74	5.28	16.97	8.13	25	16.34	22.53
10.0	CL-ML	26.76	5.68	16.97	8.98	35	18.71	24.68
12.5	CL	27.68	7.33	16.97	9.64	31	17.95	24.26
15.0	CL	27.69	7.65	17.07	11.11	25	17.68	24.89
17.5	CL-ML	27.28	6.62	17.07	12.01	36	18.05	25.17
20.0	CL	30.69	8.04	17.27	12.35	30	17.87	24.69

External stability

Generally, the external stability of a retaining system is considered as global and sliding stability. However, in soldier-piled excavation analysis, the sliding stability is neglected due to the base fixity. In the current study, the FS against global stability, which is represented with FS_G, was evaluated using the finite element strength reduction analysis. The essence of the FEM with the shear strength reduction technique is the reduction of the soil strength parameters until the soil fails. The factored shear strength parameters c'_f and φ'_f are therefore given by:

$$c'_f = \frac{c'}{FS_G} \tag{2}$$

$$\varphi'_f = \arctan\left(\frac{\tan\varphi'}{FS_G}\right) \tag{3}$$

where c' and φ' represent the shear strength parameters of the soil.

Serviceability

The maximum lateral displacement of soldier-piled excavation is one of the most important components of the serviceability limit state and hence must be controlled strictly. For this purpose, the maximum lateral displacement should not be greater than the maximum allowable lateral displacement. FS

Table 3 Geotechnical soil properties from BH.2

Depth (m)	Classification	LL (%)	PI (%)	γ_{mean} (kN/m ³)	ω_c (%)	SPT	Friction angle (Deg.)	Cohesion (kN/m ²)
2.5	CL-ML	25.00	5.15	16.77	7.61	23	14.77	20.9
5.0	ML	24.84	6.38	16.77	7.83	24	15.83	21.5
7.5	CL-ML	25.31	6.88	16.87	8.31	22	17.09	22.8
10.0	CL-ML	25.12	6.80	16.87	9.75	34	17.46	25.9
12.5	CL-ML	24.57	5.77	17.07	10.02	33	17.78	26.2
15.0	CL	26.76	6.53	17.17	10.85	30	17.36	25.4
17.5	CL-ML	24.64	5.54	17.36	11.93	38	18.76	27.1
20.0	CL	24.68	5.05	17.46	12.52	26	16.93	22.8

against this failure mode (FS_{LD}) is defined as (Burland et al. 1981):

$$FS_{LD} = \frac{R_{LD}}{\delta_{\text{max}}} \tag{4}$$

where R_{LD} is the maximum allowable lateral displacement and δ_{max} is maximum lateral soldier-piled excavation displacement obtained from the elasto-plastic analysis. It is common to use the value of 0.5% of the excavation depth for maximum allowable displacement as a governing criterion for the safety of the works and neighboring structures (Zhang et al. 2015).

Structural

The structural limit state of soldier piles can be subdivided into shear force and bending moment stability. FS against shear force (FS_{SF}) can be defined as (Burland et al. 1981):

$$FS_{SF} = \frac{R_S}{S_{\text{max}}} \tag{5}$$

In which R_S is a shear force capacity of soldier piles, and S_{max} is the estimated maximum shear force of soldier piles. Also, the FS for bending moment (FS_{BM}) can be expressed as (Burland et al. 1981):

Table 4 Properties of the model in dimension sensitivity analysis

Case no.	1	2	3	4	5
Dimension (m) (length * height)	30*16	34*20	42*24	50*28	55*32

$$FS_{BM} = \frac{R_M}{M_{max}} \tag{6}$$

where R_M is a bending moment capacity of soldier piles and M_{max} is the obtained maximum moment of soldier piles.

Modeling of unsaturated condition

Identification of the behavior of unsaturated soils is pivotal to address the geotechnical problems, including stability analysis of the retaining system located above ground water table (GWT) (Tekinsoy et al. 2004). Shear strength, which is the most important parameter affecting the behavior of unsaturated soil, can be estimated directly or indirectly (Garven 2006). The direct approach is often more complicated, costly, and time-consuming compared to the indirect approach (Assouline et al. 1998; Fredlund et al. 2002). The indirect approaches can be classified into two categories, namely effective stress method and method based on two independent state variables (Johari and Gholampour 2018). Shear strength at failure (τ_f) in the effective stress method is given by:

$$\tau_f = c' + \sigma' \tan \varphi' \tag{7}$$

where σ' , c' , and φ' are effective stress, cohesion, and friction angle, respectively. The Bishop’s formulation is used in this paper as follows (Bishop 1959):

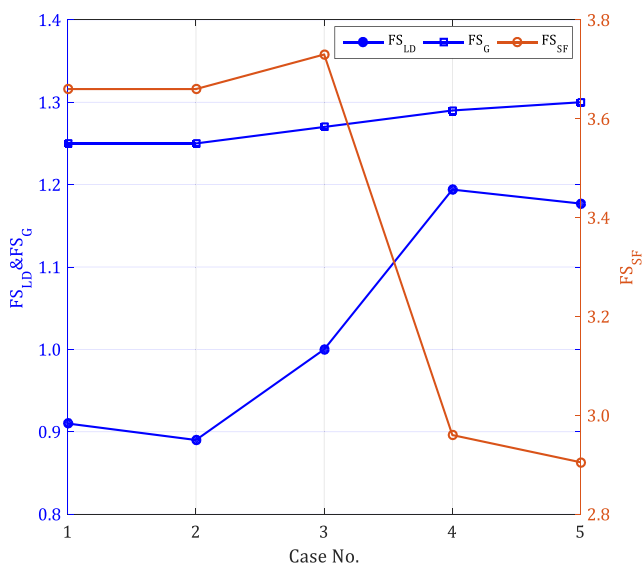


Fig. 5 Dimension sensitivity analysis

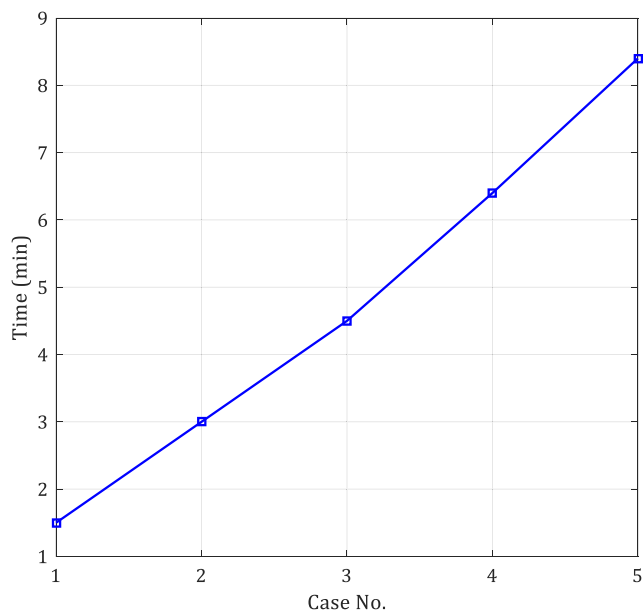


Fig. 6 Required time for one simulation

$$\sigma' = (\sigma - u_a) + \chi(u_a - u_w) \tag{8}$$

where σ is total stress, and u_a and u_w are the pore air and water pressure. $(u_a - u_w)$ is matric suction and χ is an effective stress parameter. Among various existing expressions, the one proposed by Vanapalli et al. (1996) seems to be one of the most appealing for estimating the effective stress parameters.

$$\chi = \frac{\theta_w - \theta_r}{\theta_s - \theta_r} \tag{9}$$

in which θ_w is the water content at the considered matric suction, θ_s is the saturated water content, and θ_r is the residual water content.

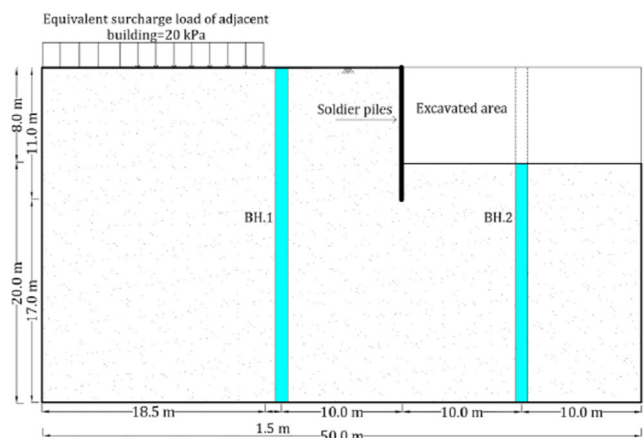


Fig. 7 Soldier-piled excavation geometry and borehole location (section 1-1)

Table 5 Properties of soldier piles applied in the modeling

D (m)	Distance (m)	f_c (MPa)	EI (kN.m ²)	EA (kN)	Υ (kN/m ³)	Poisson's ratio	Shear capacity (kN)	Moment capacity (kN.m)
0.6	1	25	149,425	6,641,100	23.80	0.15	183.37	63.59

Estimation of soil water retention curve

As described in the previous section, matric suction provides a considerable contribution to shear strength. An efficient tool to measure matric suction is the soil water retention curve (SWRC), which demonstrates a soil's ability to retain and release water as it is subjected to different suctions, with no necessity of direct method equipment. There are several methods, including direct and indirect methods, to obtain the SWRC of a particular soil, which is significantly affected by pore shape, from grain size distribution (GSD) for different depths, the particle-size distribution and the specific surface area (Johari and Golkarfard 2018). Several empirical methods have been proposed to overcome the excessive cost and time associated with a direct method. Among empirical methods, Arya and Paris' (1981) method is a prominent one for predicting the SWRC from particle-size data. Based on the advantages and capabilities of this method, the modified form of it (Arya et al. 1999) was implemented in the current study. The model first translates a particle-size distribution into a pore-size distribution. Then, the cumulative pore volumes corresponding to progressively increasing pore radii are divided by the sample bulk volume to give the volumetric water contents, and the pore radii are converted to equivalent soil water pressures using the equation of capillarity. This model offered regression fitting parameters (i.e., a and b) for limited soil type from a different region, which may lead to less accurate prediction. The great influence of SWRC fitting parameters on stability (Nguyen et al. 2019) and the intention to use the proposed model in a case study made it desirable to estimate them for the city of the case study. To tackle the shortcomings associated with this model, the work of the senior author (Johari et al. 2011) was used in this study. The soil samples from 14 different locations in the city of Shiraz were tested and their SWRCs were determined using a pressure plate apparatus. To determine the fitting parameters of each sample, some of which are presented in the Appendix (Figs. 41 and 42), the model was fitted to the experimental curve. For each type of soil, the mean value of fitting parameters which are summarized in Table 13 in the Appendix was utilized to determine the SWRC in case study.

Table 6 The soil parameters applied in the deterministic analysis

γ_{mean} (kN/m ³)	ω_{mean} (%)	Friction angle (Deg.)	Cohesion (kN/m ²)	Modulus of elasticity (kPa)	Poisson's ratio
17.0	9.80	17.20	23.10	30,000	0.35

System reliability analysis

The variability of the soil properties, even within homogeneous layers, is the most dominating source of uncertainty in geotechnical engineering. Hence, considering the spatial variability of soil properties by using the appropriate method is crucial. The RFEM offers a useful tool to incorporate spatial variability of soil properties into stability analysis by combining a random field with the FEM (Griffiths and Fenton 2004).

Random field theory

The theory of random fields, which was achieved by Vanmarcke (1983), is a powerful and rigorous method for modeling the variability of soil properties. The set of random variables at all positions within the entire volume of the soil is mentioned as a random field according to a correlation between adjacent random variables. It is expected that the correlation value decreases by increasing the distance between the two positions. This distance in which the soil parameters are rationally well-correlated to its neighbors is called the autocorrelation length (l).

The spatial correlation of soil parameters can be characterized by their correlation function within the framework of random fields (Vanmarcke 1983). The correlation function of specified soil properties can be computed from known data of the properties at various positions (Baecher and Christian 2005). The correlation between two different random variables (e.g., x_1 and x_2) is measured by a correlation function defined as follows (Ahmed 2012):

$$\rho(x_1, x_2) = \frac{1}{\sigma_{x_1} + \sigma_{x_2}} E[(x_1 - \mu_{x_1})(x_2 - \mu_{x_2})] \quad (10)$$

in which x_1 and x_2 might be the values of two different properties or the values of the same property at two different locations. σ_{x_i} and μ_{x_i} are, respectively, the standard deviation and the mean value of the variable x_i ($i = 1, 2$). In the current research, the Markov correlation function was utilized to characterize the spatial autocorrelation of

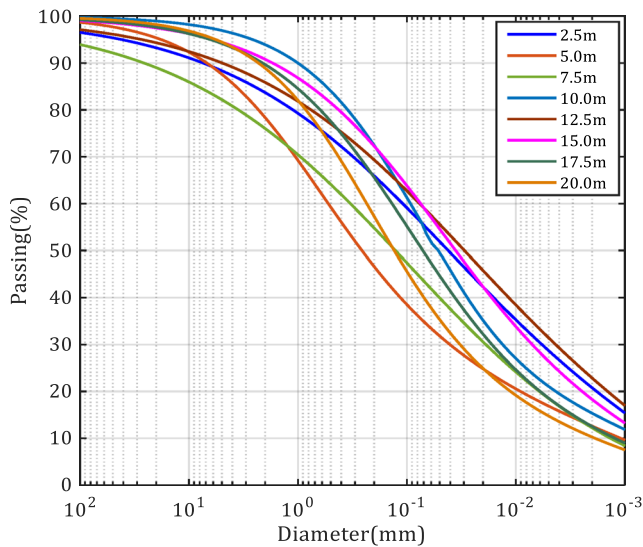


Fig. 8 The GSD for BH.1 in different depths

the soil properties (Nguyen and Likitlersuang 2019) as:

$$\rho(\tau_x, \tau_y) = \exp\left\{-\frac{2\tau_x}{l_x}\right\} \exp\left\{-\frac{2\tau_y}{l_y}\right\} \quad (11)$$

where τ_x and τ_y are the differences between the horizontal and vertical directions of any two points in the random field, respectively, and l_x and l_y are the autocorrelation lengths in the horizontal and vertical directions, respectively.

Due to the significant influence of the autocorrelation lengths on stability of geotechnical problems in unsaturated state (Nguyen et al. 2017), it would be more appropriate to evaluate them from known data. The sample autocorrelation function (ACF) can be a simple and useful tool for this purpose. The ACF is the graph of the sample autocorrelation at lag k , r_k , for lags $k = 0, 1, 2, \dots, m$, where m is the maximum

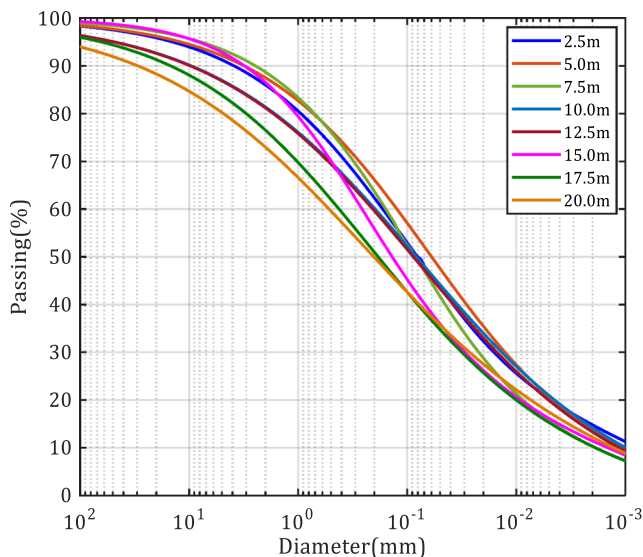


Fig. 9 The GSD for BH.2 in different depths

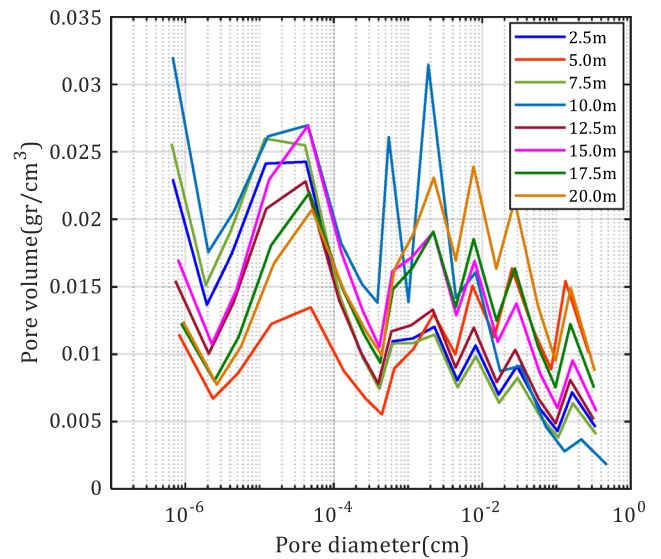


Fig. 10 The PSD for BH.1 in different depths

number of lags allowed for obtaining reliable estimates. The r_k is defined as follows (Jaksa 2013):

$$r_k = \frac{\sum_{i=1}^{N-k} (X_i - \bar{X})(X_{i+k} - \bar{X})}{\sum_{i=1}^N (X_i - \bar{X})^2} \quad (12)$$

where X_i and X_{i+k} are the values of the variable at points i and $i+k$ respectively, and \bar{X} is the mean value of the variable. Vanmarcke (1983) suggested that autocorrelation lengths can be determined by fitting one of the models to the sample ACF, as given in Table 1, where Δz is the depth interval.

The numerical methods such as finite element have discrete nature; hence, a continuous-parameter random field must also be discretized into random variables.

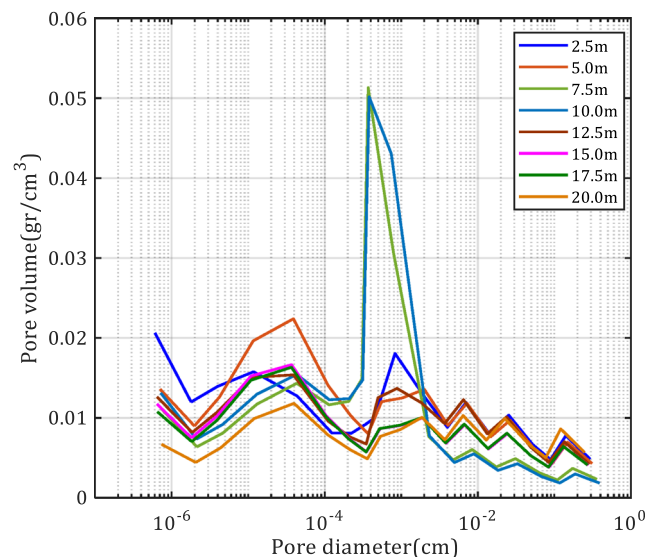


Fig. 11 The PSD for BH.2 in different depths

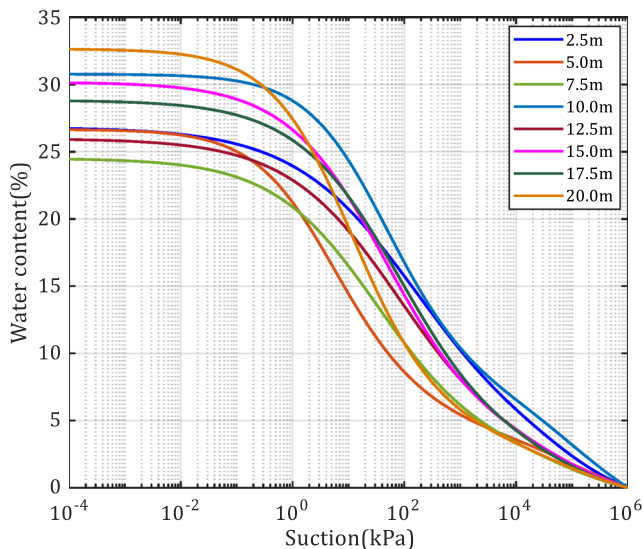


Fig. 12 The SWRC for BH.1 in different depths

This process is commonly known as the discretization of a random field. Various methods have been presented for the discretization of a random field (e.g., Li and Der Kiureghian 1993). In the current research, the covariance matrix decomposition approach (Fenton and Griffiths 2003) was utilized for the discretization of the random field.

The system reliability approach

Physical systems which are consisted of several components can be categorized as series, parallel, and combined systems (Johari and Lari 2017). In the case of a series system, the failure of each component led to the failure of the whole system. However, the parallel system would not fail unless all failure modes occur. Since

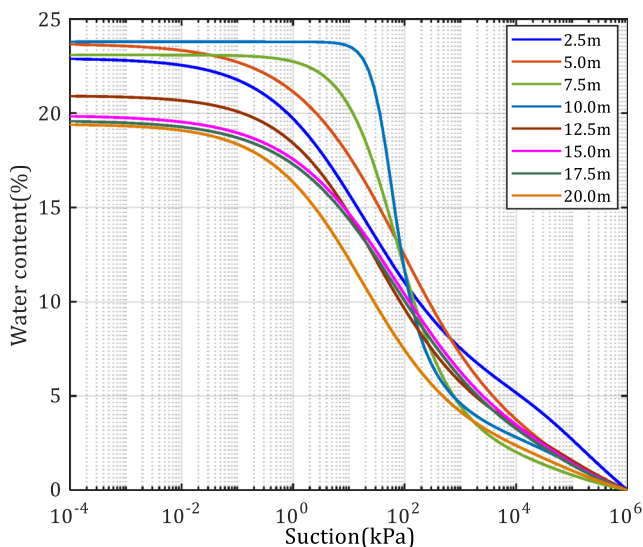


Fig. 13 The SWRC for BH.2 in different depths

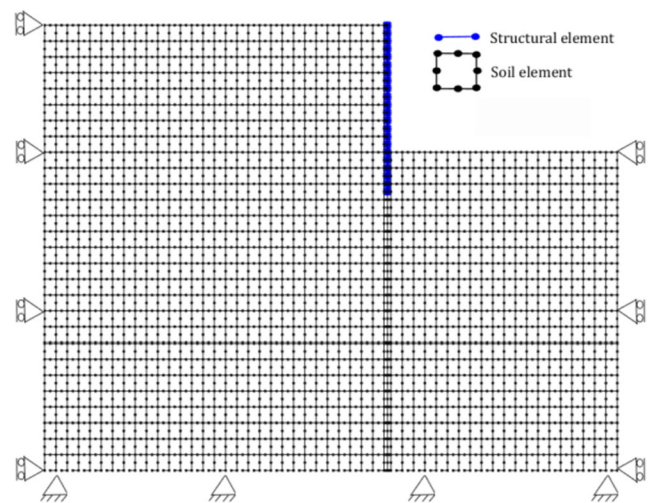


Fig. 14 Finite element mesh and boundary conditions

the failure of at least one component of soldier-piled excavation leads to the failure of the whole retaining system, it can be modeled as a four-component series system (i.e., global, lateral displacement, shear force and bending moment). Several approaches have been presented for combining the components of parallel systems (i.e., the intersection of component events), series systems (i.e., a union of the component event), and combined systems (Genz and Bretz 2002; Pandey and Sarkar 2002). To tackle the problems associated with the previous approaches, Kang and Song (2010) proposed an efficient method (SCM) in which the reliability of the components is first computed, and the components are subsequently combined into equivalent components two at a time until the full system reliability is obtained. Distinct superiority of the SCM over the others is minimizing the complexity of logical operation as it involves only two components in each process.

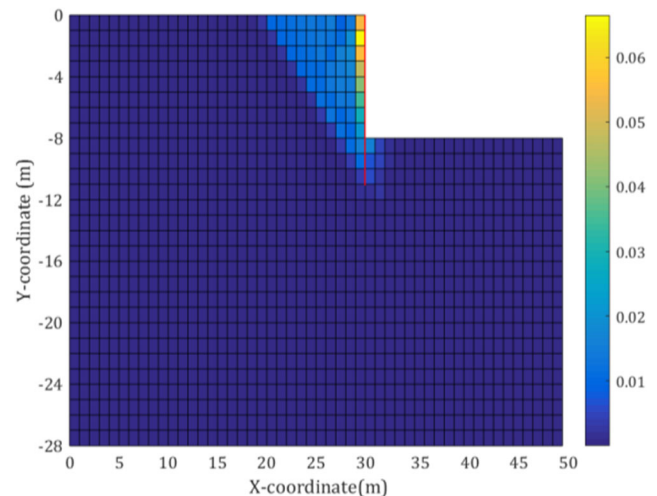
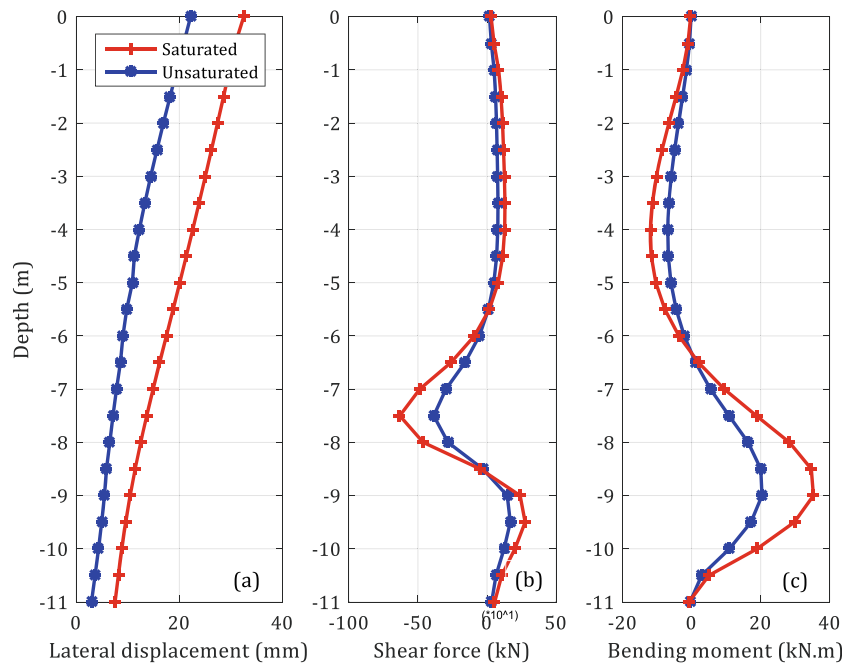


Fig. 15 The shear strain of soldier-piled excavation

Fig. 16 Simulated excavation-induced responses of the soldier piles proposed model. (a) Lateral displacement. (b) Shear force. (c) Bending moment



Consider compounding two components E_1 and E_2 coupled by union into a single equivalent event E_{1or2} . For example, this compounding can appear in a series system, and can be compounded as follows:

$$\frac{P(E_1 \cup E_2 \cup \dots \cup E_{10})}{P((E_1 \cup E_2 \cup E_3) \cap (E_4 \cup E_5 \cup E_6))} = \frac{P(E_{1or2} \cup E_3 \cup \dots \cup E_{10})}{P((E_{1or2} \cup E_3) \cap (E_4 \cup E_5 \cup E_6))} \quad (13)$$

First, using De Morgan's rule and the symmetry of the standard normal distribution, the reliability index of the compound event E_{1or2} is obtained by:

$$\begin{aligned} \beta_{1or2} &= -\Phi^{-1}[P(E_1 \cup E_2)] = -\Phi^{-1}\left[P(\bar{E}_1 \cap \bar{E}_2)\right] \\ &= \Phi^{-1}\left[P(\bar{E}_1 \cap \bar{E}_2)\right] \\ &= \Phi^{-1}\left[\Phi(\beta_1)\Phi(\beta_2) + \int_0^{\rho_{1,2}} \varphi_2(\beta_1, \beta_2, \rho) d\rho\right] \quad (14) \end{aligned}$$

where β_1 and β_2 are the reliability indexes of E_1 and E_2 , respectively, and $\rho_{1,2}$ is the correlation coefficient between the standard normal random variables Z_1 and Z_2 , which respectively represent E_1 and E_2 . Next, the aim is to find the

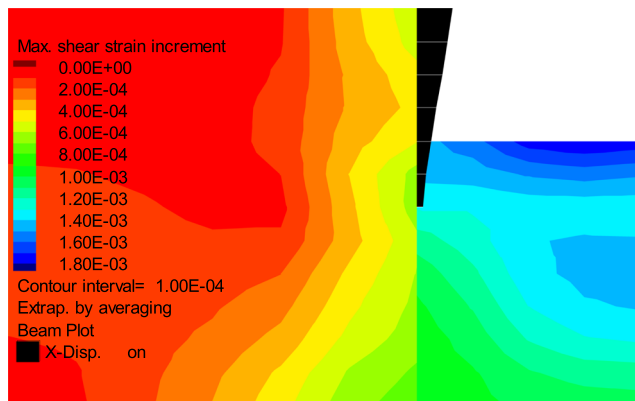


Fig. 17 Simulated excavation-induced lateral displacement of the soldier piles in the unsaturated state by FLAC

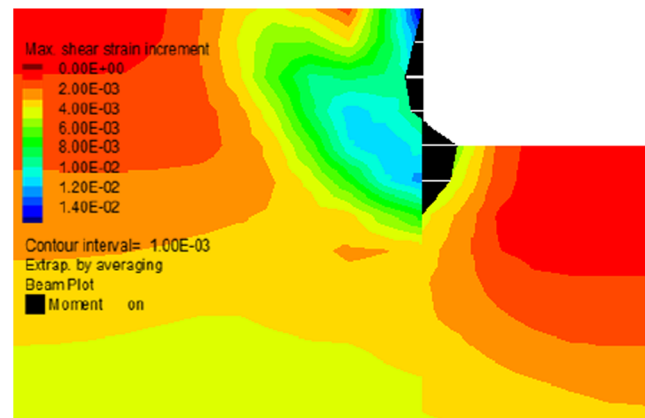


Fig. 18 Simulated excavation-induced bending moment of the soldier piles in the saturated state by FLAC

Table 7 Comparison of the excavation-induced responses of the soldier piles in saturated state

Models	Maximum lateral displacement (mm)	Maximum shear force (kN)	Maximum bending moment (kN.m)
Proposed model	33.2	61.8	35.3
FLAC	32.9	62.4	36.2

equivalent correlation coefficient $\rho_{(1or2),k}$ that would provide the same estimate on the probability of the following event $\Omega_u = [(Z_1 \leq -\beta_1) \cup (Z_2 \leq -\beta_2)] \cap (Z_k \leq -\beta_k)$ after compounding, i.e.,

$$\int_{\Omega_u} \varphi_3(z_1, z_2, z_3; \rho_{1,2}, \rho_{1,k}, \rho_{2,k}) dz = \Phi_2(\beta_{1or2}, -\beta_k; \rho_{(1or2),k}) \tag{15}$$

where Ω denotes the domain of a system event defined in the space of n standard normal random variables.

Using the decomposition and approximation used in conditional probabilities, Eq. (15) is approximated as

$$1 - \Phi_2(\beta_{1|k}, \beta_{2|k}; \rho_{1,2|k}) = \Phi(-\beta_{(1or2)|k}) \tag{16}$$

where $\Phi_2(\cdot)$ and $\Phi(\cdot)$ respectively denote the joint cumulative distribution function (CDF) of the bivariate standard normal distributions and the cumulative distribution function of the standard normal distribution.

$$\beta_{(1or2)|k} = (\beta_{1or2} - \rho_{(1or2),k} A) / \sqrt{1 - \rho_{(1or2),k}^2} B \tag{17}$$

where $A = \varphi(-\beta_k) / \Phi(-\beta_k)$ and $B = A(-\beta_k + A)$ in which $\varphi(\cdot)$ denotes the probability density function (PDF) of the standard normal distribution.

The bivariate CDF in Eq. (16) can be computed by performing the single-fold numerical integration as follows:

$$\Phi_2(\beta_{1|k}, \beta_{2|k}; \rho_{1,2|k}) = \Phi(\beta_{1|k}) \Phi(\beta_{2|k}) + \int_0^{\rho_{1,2|k}} \varphi_2(\beta_{1|k}, \beta_{2|k}; \rho) d\rho \tag{18}$$

where at each compounding, Eqs. (16) and (17) are solved numerically for $\rho_{(1or2),k}$ $k = 3, \dots, n$ in which n is the current total number of components in the system during a sequential compounding process with the constraint $-1 \leq \rho_{(1or2),k} \leq 1$.

Execution process of system reliability analysis of soldier-piled excavation

In prior sections, the processes for determining the shear strength parameters of unsaturated soil and finite element modeling and generating random fields were presented. The main emphasis in the current section is on the implementation of the proposed reliability analysis for soldier-piled excavation in unsaturated soils. The execution process is schematically illustrated in Fig. 2, and can be described as follows:

- (1) Extracting the required data from boreholes and discretization of the domain
- (2) Obtaining the SWRC from GSD for different depths
- (3) Generating random fields for considered parameters (i.e., water content, cohesion, friction angle, and unit weight of the soil excavation domain)
- (4) For each element:
 - (a) Calculating the suction stress by ω_c and SWRC related to the element’s depth
 - (b) Estimating the total stress by considering soil unit weight as gravity loads
 - (c) Determining the effective stress using the estimated suction stress and total stress
 - (d) Estimating the shear strength of unsaturated soil
- (5) Performing finite element elasto-plastic and strength reduction analysis to determine the FS of the failure modes (i.e., FS_G, FS_{LD}, FS_{SF}, and FS_{BM})
- (6) Repeating steps (3) to (5) as many as the number of simulations in order to obtain the reliability and statistics properties for all the failure modes
- (7) Conducting system reliability analysis to obtain the overall reliability of the system, instead of several partial reliabilities indexes

Table 8 Sensitivity analysis of input parameters

Studied parameters	Cohesion (kPa)	Friction angle (Deg.)	Unit weight (kN/m ³)	Poisson’s ratio	Modulus of elasticity (kPa)
Change in FS (%)	5.8	4	8.8	0.2	0.2

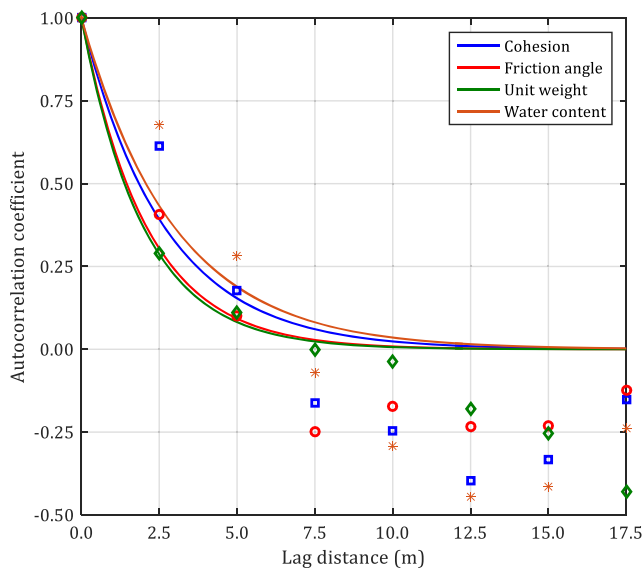


Fig. 19 Sample and model ACF of BH.1

Case study

A case study of the soldier-piled excavation in the unsaturated state is presented to bring out the performance of the suggested method and validation of MATLAB code. For this purpose, deterministic analysis was followed by a reliability evaluation to take in to account the variability of soil properties and unsaturated state. In the next step, system reliability analysis was conducted to offer a single index for quantifying the overall reliability of the system, instead of several partial reliabilities indices.

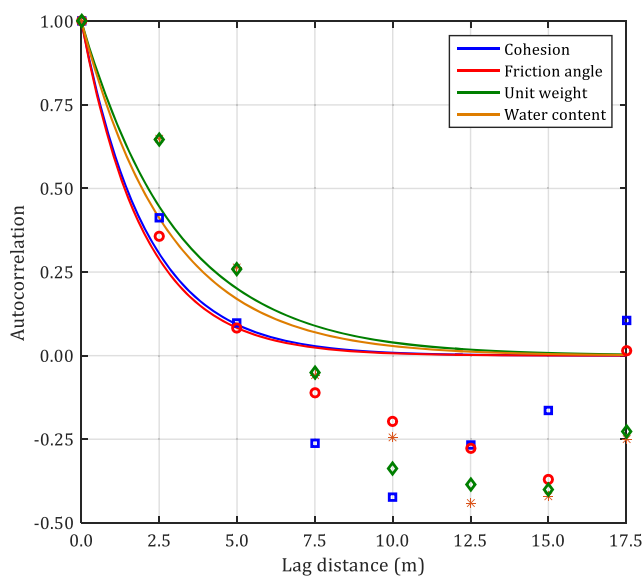


Fig. 20 Sample and model ACF of BH.2

Table 9 Parameter *b* estimated from fitted model

Parameters	$b_{(BH.1)}$	$b_{(BH.2)}$
Cohesion	2.67	2.03
Friction angle	2.10	2.01
Unit weight	2.00	2.90
Water content	2.99	2.96

The site characterization and geotechnical soil properties

The intended site is situated in Shiraz, a city in Iran, as illustrated in Fig. 3. The key aim for choosing the site was that it mainly contains fine-grained soil in which unsaturated state can cause significant suction and consequently affect the stability of retaining systems. Furthermore, the uniform geometry of the intended excavation is appropriate for plane strain conditions. To specify the soil properties of the site, two boreholes (i.e., BH.1 and BH.2) with 20 m depth are drilled which their relative locations are illustrated in Fig. 4. The soil properties are obtained through the field and laboratory tests. Soil properties of BH.1 and BH.2 are summarized in Tables 2 and 3, respectively.

Modeling and verification

A finite element-based program is coded in MATLAB to estimate FS, deflection, and internal forces of soldier piles. The program is for two-dimensional plane strain analysis of elastic perfectly plastic soils with a Mohr-Coulomb failure criterion utilizing eight-node quadrilateral elements with reduced integration (four Gauss points per element) in the gravity loads generation, the stiffness matrix generation, and the stress redistribution phases of the algorithm. The soil is initially assumed to be elastic, and the model generates normal and shear stresses at all Gauss points within the mesh. These stresses are then compared with the Mohr-Coulomb failure criterion. If the stresses at a particular Gauss point lie within the Mohr-Coulomb failure envelope, then that location is assumed to remain elastic. If the stresses lie on or outside the

Table 10 The mean and standard deviation of considered stochastic parameters

Parameters	Mean (μ)	Standard deviation
Cohesion (kPa)	23.8	3.02
Friction angle (Deg.)	17.2	1.21
Unit weight (kN/m ³)	17.0	0.23
Water content (%)	9.80	1.91

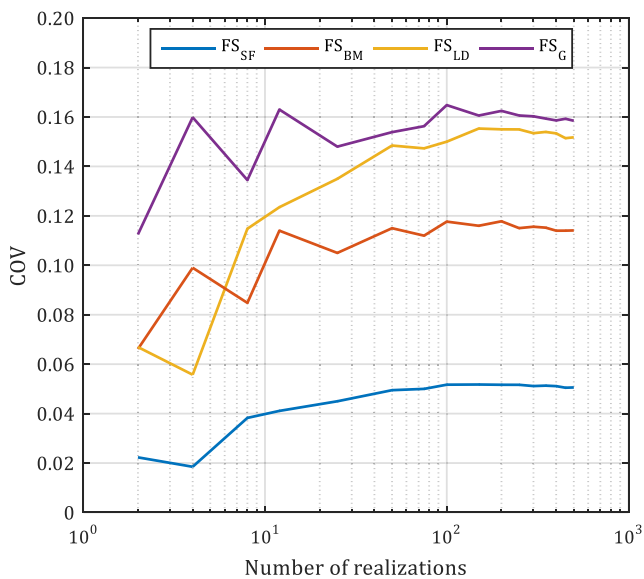


Fig. 21 Sensitivity analysis of number of realization in unsaturated state

failure envelope, then that location is assumed to be yielding. Global shear failure occurs when a sufficient number of Gauss points have yielded to allow a global failure mechanism to develop, causing the displacements in the excavation to increase dramatically.

The accuracy and computational efficiency are critical factors in FEM modeling. Although the accuracy of the FEM model improves slightly with enlarging the dimensions of it, it leads to a significant increase in computation time and cost. The problem is exacerbated in the case of stochastic analysis in which the process is repeated several hundred times. Hence, a sensitivity analysis is needed to evaluate the influence of the model dimensions on responses of soldier-piled excavation. To do this, the problem was modeled with various dimensions, as tabulated in Table 4. The results of dimension sensitivity analysis are presented in Fig. 5. Also, the required time for one realization is illustrated in Fig. 6. It can be seen that the rate of variation of FSs is significantly different before and after case no. 4. On the other hand, enlarging the dimensions of the problem greatly increases the computation time. Hence,

case no. 4 was considered as a model geometry since it was more efficient than others in terms of accuracy and computation time. Also, the geometry of the model was verified by the study of Brinkgreve et al. (2014), which revealed that the minimum distance between the retaining system and excavated-side boundary is 3 to 5 times the embedment depth of the soldier piles. Furthermore, the minimum distance between the retaining system and the unexcavated-side boundary was 2 to 3 times of the soldier piles length while the minimum distance between the bottom of the soldier piles and the bottom boundary was soldier piles length. The bottom boundary was restrained from both horizontal and vertical movements, while the left- and right-side boundaries were only restrained horizontally.

The general conditions of the studied retaining system, such as its model geometry, surcharge load, and boreholes locations are illustrated in Fig. 7 through cross-section 1-1 of Fig. 4. The properties of soldier piles and soil that are used in the deterministic analysis are given in Tables 5 and 6, respectively, while the particle density was considered 2.65 g/cm³.

The suction which is applied in the analysis was calculated as a continuous one-dimensional profile. The suction profile was estimated from SWRCs which were obtained for different depth using a physico-empirical model (Arya et al. 1999). For this purpose, the PSDs were extracted from GSDs which were obtained by fitting the Fredlund et al. (2000) equation to the measured data. Then, the SWRCs were estimated through the mentioned approach in the “Methodology of analysis” section by fitting the Fredlund and Xing (1994) equation to the experimental data.

The GSDs, PSDs, and the related SWRCs for the soil samples of BH.1 and BH.2 are shown in Figs. 8, 9, 10, 11, 12, and 13, respectively. Using the estimated suctions, the stability analysis was conducted deterministically and the FS_G of 1.3 and 2.2 was determined with and without considering unsaturated state, respectively. As is was expected and has been stated in the literature (e.g., Li et al. 2006), considering the unsaturated state in stability analysis led to improving FSs. Although the soldier-piled excavation was stable (i.e., FS >

Fig. 22 The domain random field of 1th realization for cohesion (kN/m²)

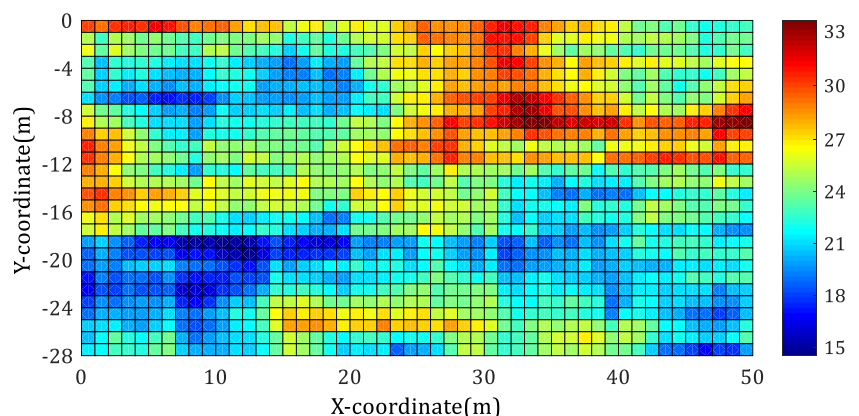
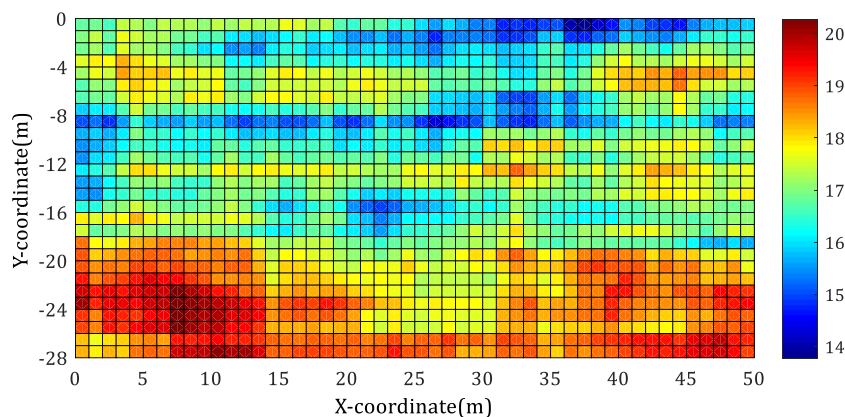


Fig. 23 The domain random field of 1th realization for friction angle (Deg.)



1) before considering suction in deterministic analysis, it was in unsafe condition based on national code, which recommended the minimum value of 1.25 for FS with respect to all failure modes.

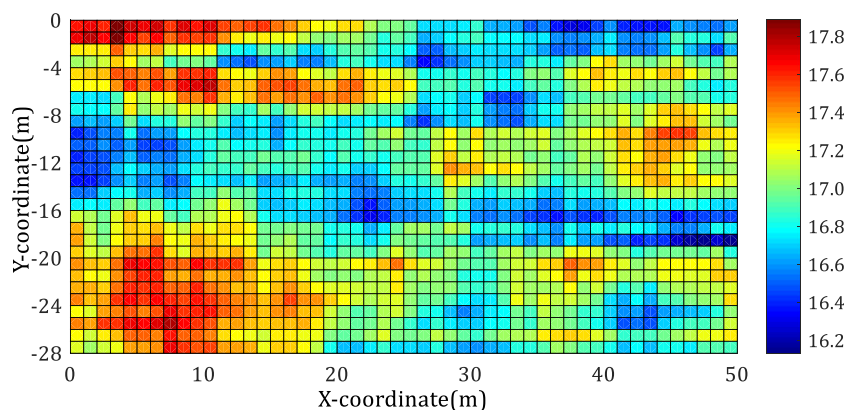
The finite element mesh with boundary conditions and the shear strain of the soldier-piled excavation are illustrated in Figs. 14 and 15, respectively. Also, the simulated profiles of lateral deflection, bending moment, and shear forces of soldier piles are shown in Fig. 16.

For the verification, the deterministic analysis results of the coded program in the saturated and unsaturated state were compared with those from the commercial finite difference software package FLAC. For this purpose, a soldier-piled excavation with the same geometry and boundary condition was modeled by two methods. As indicated in Figs. 17 and 18 and Table 7, the results showed a good agreement with the coded program.

Reliability analysis

To conduct a reliability analysis of soldier-piled excavation, random fields were generated for unsaturated effective parameters of soil. To identify these parameters, in addition to ω_c which play key roles in controlling the behavior of unsaturated soils, a sensitivity analysis was conducted. To do this, each

Fig. 24 The domain random field of 1th realization for the unit weight (kN/m^3)

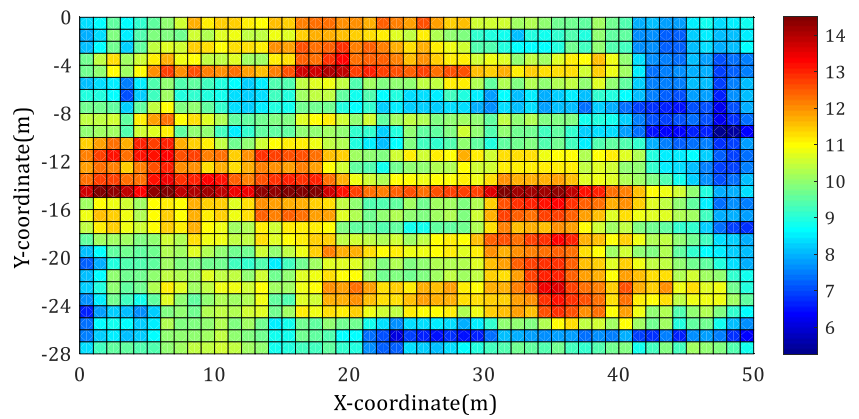


parameter was increased by 10% of its value, while other input parameters were kept constant. Table 8 indicates the changes in the FS due to sensitivity analysis. It can be seen that unit weight is the most effective parameter on the FS, while Poisson's ratio and modulus of elasticity have no significant effect on it. Also, the next effective parameter is cohesion and friction angle, respectively.

Due to the availability of sufficient soil data in a vertical direction, the l_y was estimated using the ACF, and single exponential curve model (i.e., model no. 2 in Table 1) described in the "Random field theory" section. The ACFs and the fitted model for the soil parameters from BH.1 and BH.2 are illustrated in Figs. 19 and 20, respectively. The related fitting parameter values for different soil properties are tabulated in Table 9. According to the results, the l_y was considered 5.0 m as twice the mean value of parameter b obtained from boreholes, which was within the range of 0.1–7.2 m estimated by various studies (Cami et al. 2020). Furthermore, l_x was considered as 25 m due to the fact that the horizontal correlation length is usually much larger, and its influence is much less important compared with the vertical correlation length (Phoon and Kulhawy 1999).

The stochastic parameters were modeled within 3σ of difference from the mean, using truncated normal probability distribution functions with the mean and standard deviation, which are presented in Table 10. The correlation coefficient

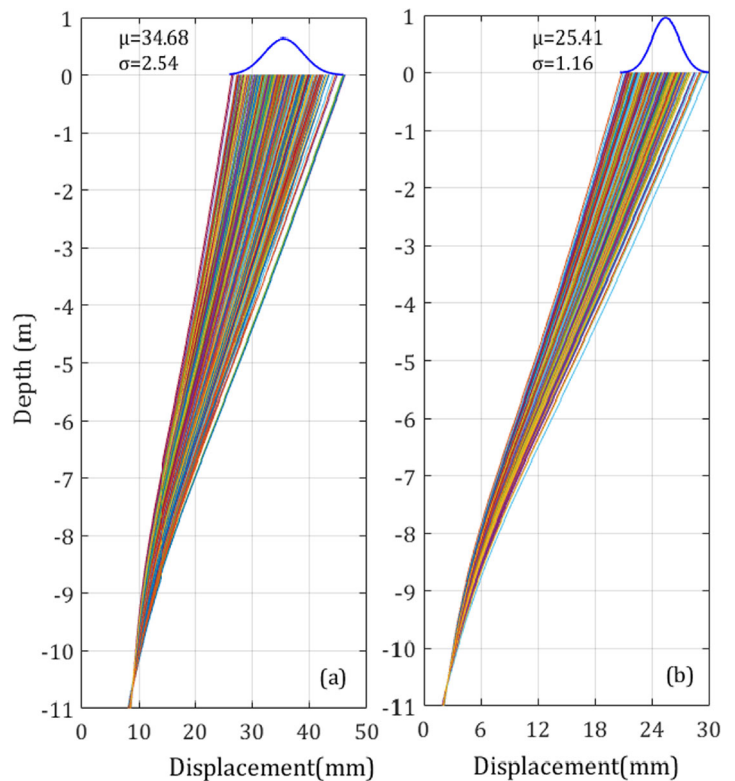
Fig. 25 The domain random field of 1th realization for water content (%)



between cohesion and friction angle was selected $\rho_{c,\phi} = -0.5$ based on previous studies (e.g., Cherubini 2000) which proposed several ranges for $\rho_{c,\phi}$, from -0.24 to -0.7 . A negative correlation means one variable may take on a large value while the other assumes a small one and vice versa. The positive correlation, which implies that both variables tend to assume either large values or small values simultaneously, between friction angle and unit weight suggested within the range of 0.1 to 0.7 (Wu 2013). In this study, this value was selected as $\rho_{\phi,\gamma} = 0.7$.

The number of realization necessary for any statistical analysis is a function of the desired precision of the analysis, the greater the number of realizations, the more precise the results are. Increasing the number of realizations beyond a certain limit, however, can be regarded as a tedious process with very little improvement in the numerical accuracy of the analysis results. Previous researchers (e.g., Huang et al. 2017; Rahman and Nguyen 2012) used statistical parameters of the system response to obtain the required number of realization, such as mean, standard deviation, and the coefficient of variation

Fig. 26 Lateral displacement uncertainties of the soldier piles due to stochastic analysis. (a) Saturated state. (b) Unsaturated state



(COV), which is defined as the ratio of the standard deviation to the mean. In this study, to estimate the effective number of realization for selected geometry, a sensitivity analysis was carried out using a COV of FS with respect to different failure modes. Figure 21 depicts the variations of calculated COV of FSs against the number of simulations. The adequate number of realizations was found to be 500, which beyond it, no significant change occurred in the value of COVs. The random field results for all parameters are depicted in Figs. 22, 23, 24, and 25.

Effects of unsaturated state on FS and reliability indices of failure modes

To evaluate the influence of the unsaturated state on FS of all failure modes, the analysis was performed with and without taking into consideration the soil suction. In the case of the saturated state, the negative pore pressure above GWT was neglected and 500 random fields were generated for random parameters except for water content (i.e., cohesion, friction angle, and unit weight). However, in an unsaturated state, random fields were generated for all random parameters due to the important role of negative pore pressure in soil shear strength. As a result of the stochastic analysis, the

uncertainties of lateral displacement, shear force, and bending moment profiles of the soldier piles for the saturated and unsaturated state are presented in Figs. 26, 27, and 28, respectively. Lognormal distributions were fitted to the variation of lateral displacement at the top of the soldier piles and at the positive and negative points of the shear force and the bending moment of them. As can be seen, by taking suction into account, the mean and standard deviation of lateral displacement decreased by 26.9% and 54.7%, respectively. Also, the mean and standard deviation of the maximum shear force decreased by about 31.6% and 64.6%, respectively. In line with the results, by considering suction, the mean and standard deviation of the maximum bending moment decreased by about 31.7% and 57.8%, respectively. These significant changes can lead to completely different outcomes in the reliability analysis.

The PDFs of FS with respect to all failure modes (i.e., global, lateral displacement, shear force and bending moment) in saturate and unsaturated states are illustrated in Figs. 29, 30, 31, and 32. The good lognormal fits were obtained for PDFs despite the use of normal probability distribution for random variables. Considering unsaturated state improves PDF of FS with respect to all failure modes by shifting from risky zone to safe zone based on Engineers, U.A.C.o. (1997). These figures

Fig. 27 Shear force uncertainties of the soldier piles due to stochastic analysis. (a) Saturated state. (b) Unsaturated state

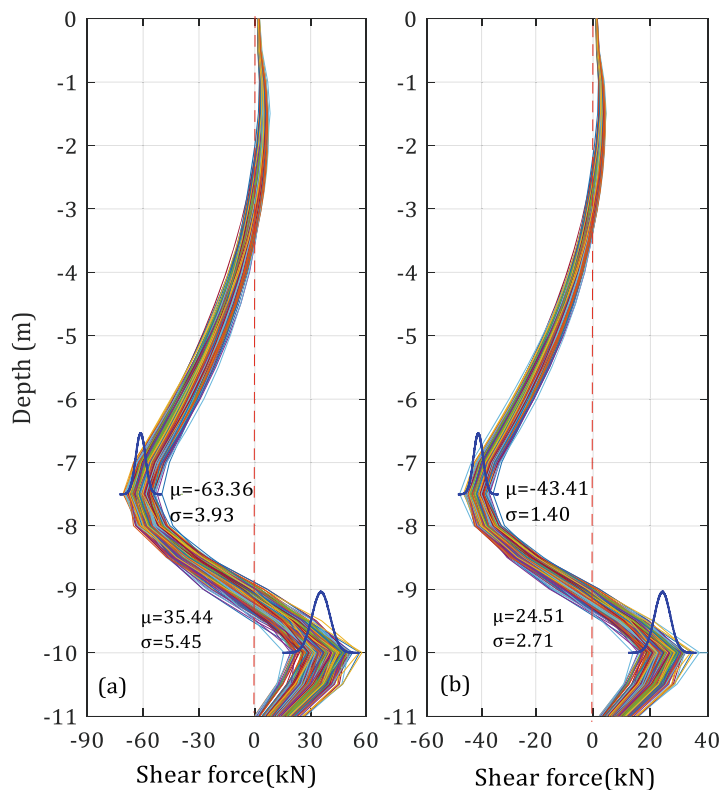
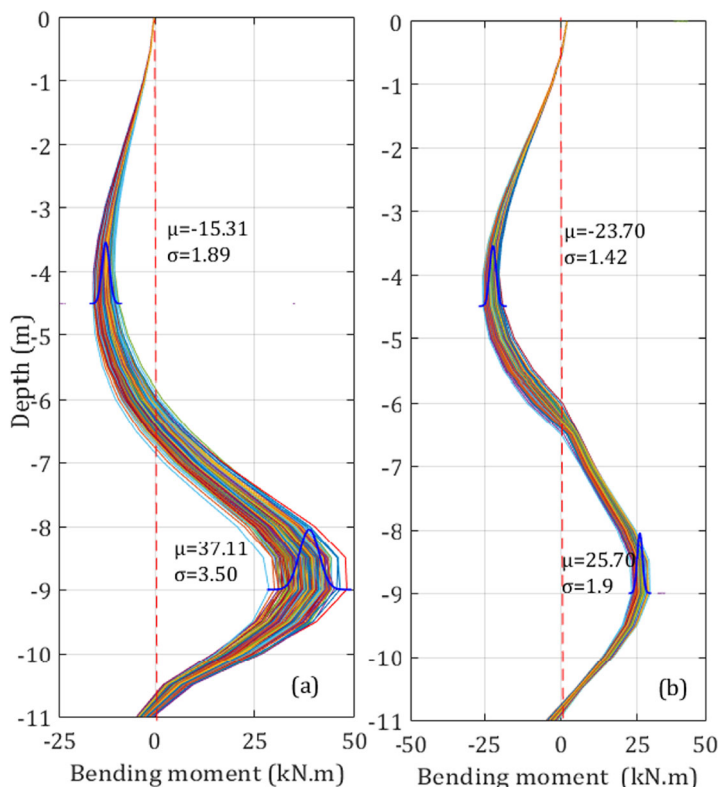


Fig. 28 Bending moment uncertainties of the soldier piles due to stochastic analysis. (a) Saturated state. (b) Unsaturated state



indicate that neglecting the unsaturated state leads to conservative design for the retaining system with the same

properties. The related statistical parameters and reliability index of all failure modes are tabulated in Table 11.

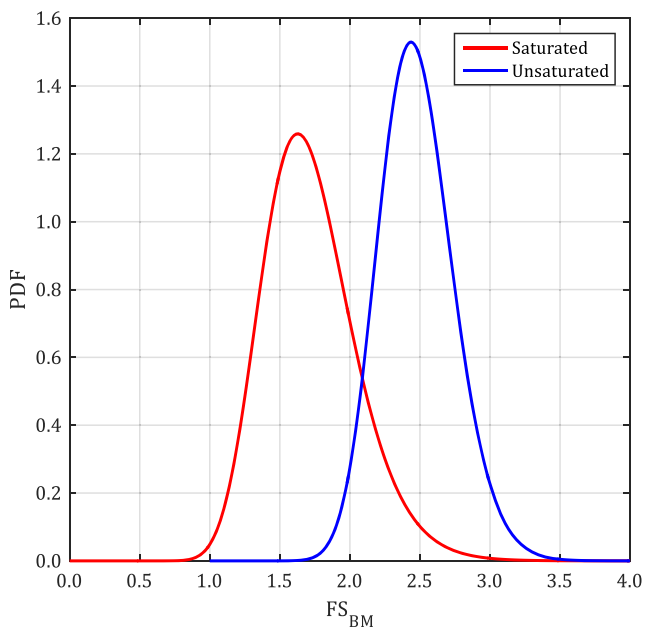


Fig. 29 Comparison of the PDF of FS_{BM} for saturated and unsaturated states

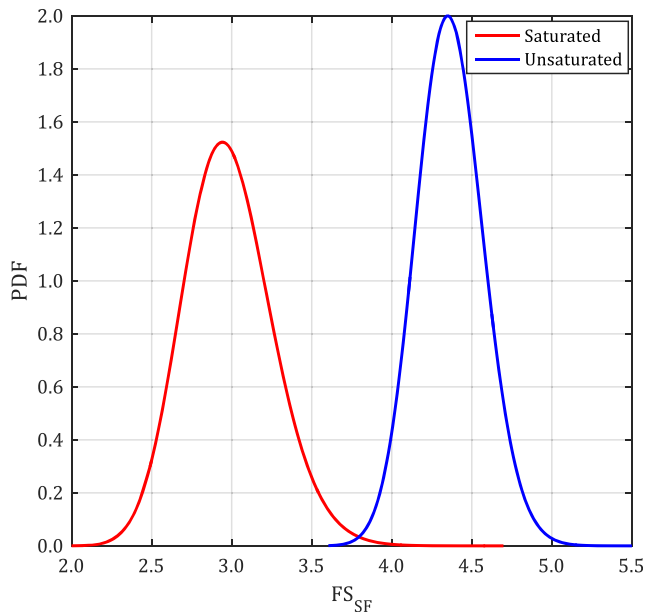


Fig. 30 Comparison of the PDF of FS_{SF} for saturated and unsaturated states

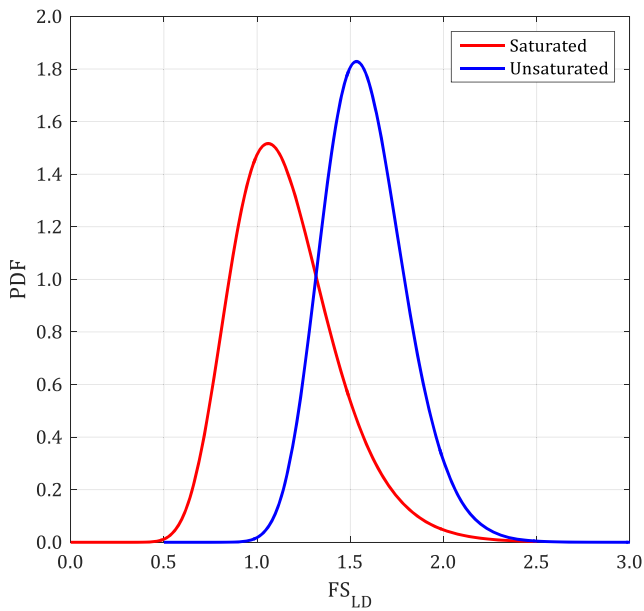


Fig. 31 Comparison of the PDF of FS_{LD} for saturated and unsaturated states

The reliability index (β) is an alternative measure of safety, or reliability, which is uniquely related to the P_f . The value of β indicates the number of standard deviations between failure and the most likely value for safety factor which may be defined for lognormal distributions as follows:

$$\beta = \frac{\ln \left[\frac{\mu}{\sqrt{1 + COV^2}} \right]}{\sqrt{\ln(1 + COV^2)}} \tag{19}$$

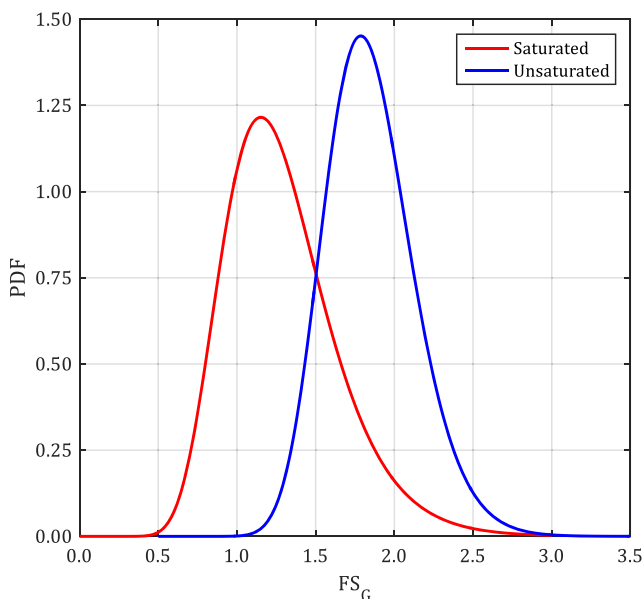


Fig. 32 Comparison of the PDF of FS_G for saturated and unsaturated states

Table 11 Statistical parameters of FS for various failure modes in a saturated and unsaturated states

Condition	Failure mode	μ	σ	β	COV (%)	P_f
Saturated	FS_{BM}	1.73	0.32	2.84	0.19	0.02
	FS_{SF}	2.93	0.31	9.99	0.11	0.00
	FS_{LD}	1.17	0.38	0.32	0.31	0.45
	FS_G	1.30	0.42	0.66	0.32	0.38
Unsaturated	FS_{BM}	2.48	0.29	8.01	0.11	0.00
	FS_{SF}	4.24	0.22	27.70	0.05	0.00
	FS_{LD}	1.58	0.28	2.91	0.15	0.03
	FS_G	1.86	0.29	3.84	0.16	0.01

Due to the symmetry of the normal distribution, P_f can be expressed as follows:

$$p_f = 1 - \Phi(-\beta) \tag{20}$$

in which Φ is the cumulative standard lognormal distribution function.

Based on the presented COV of the failure modes in Table 11, it can be seen that the uncertainty of the soil parameters has the most significant effect on the global safety factor of the excavation, while shear force failure mode is less affected than others.

To compare the failure probability of saturated and unsaturated conditions, the CDFs of FS with respect to all failure modes (i.e., global, lateral displacement, shear force, and bending moment) are plotted in Figs. 33, 34, 35, and 36. These curves can also provide a frame for the direct implementation of probabilistic and reliability analyses in the structural design process. The procedure of obtaining the required data for the purpose of structural design

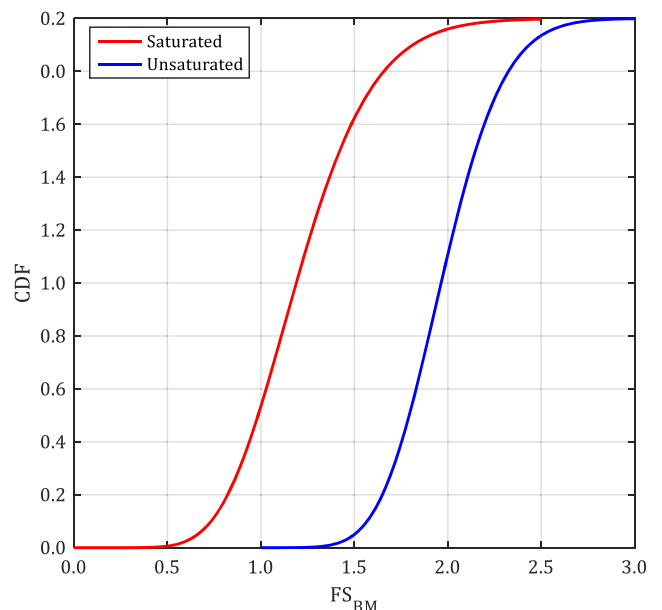


Fig. 33 Comparison of the CDF of FS_{BM} for saturated and unsaturated states

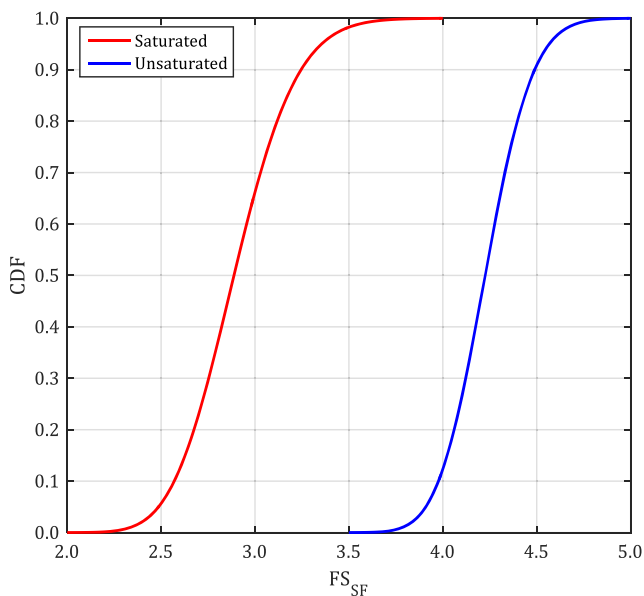


Fig. 34 Comparison of the CDF of FS_{SF} for saturated and unsaturated states

(i.e., lateral displacement, shear force, and bending moment) can be summarized as follows. First, determine the target P_f to achieve the desired performance level which can be found in the US Army Corps of Engineers (Engineers UACo 1997) and are tabulated in Table 12. Next, obtain the FS that takes on a selected value of P_f using CDF of each failure mode. Then, calculate the lateral displacement, shear force, and bending moment for the purpose of structural design using the following equations:

$$\delta_d = \frac{R_{LD}}{FS_L} \tag{21}$$

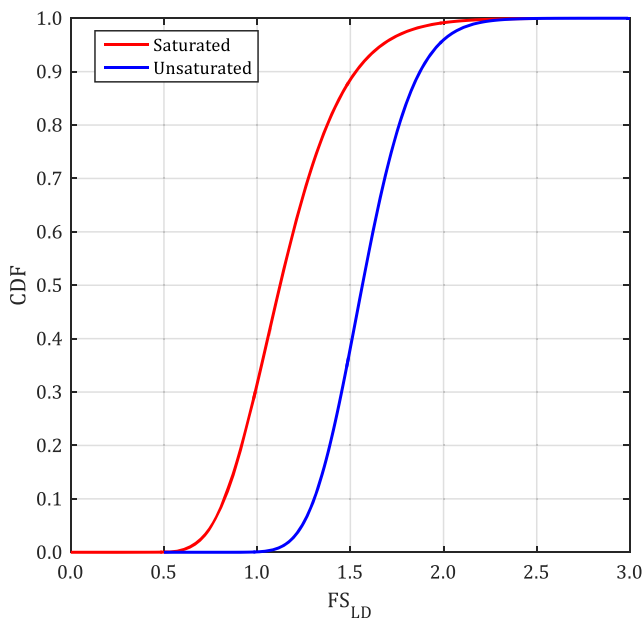


Fig. 35 Comparison of the CDF of FS_{LD} for saturated and unsaturated states

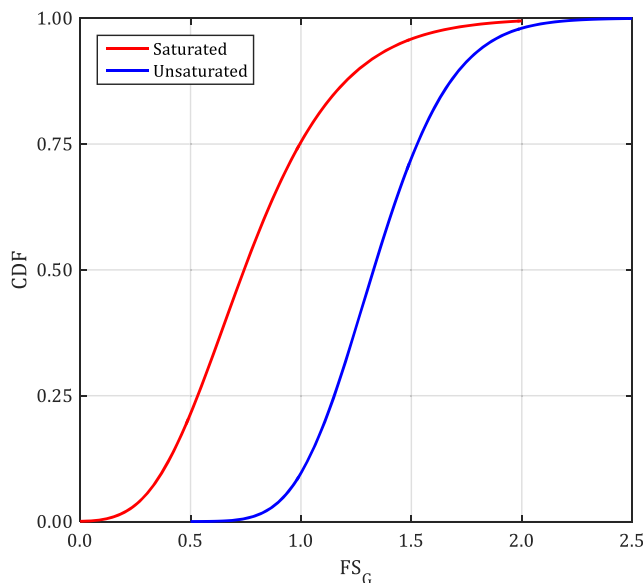


Fig. 36 Comparison of the CDF of FS_G for saturated and unsaturated states

where δ_d , S_d , and M_d are design lateral displacement, shear force, and bending moment, respectively. FS_L , FS_S , and FS_M are respectively FS with respect to lateral displacement, shear force, and bending moment failure obtained from related CDF.

System reliability analysis

The key advantage of the system modeling approach is that it provides a single index for quantifying the overall reliability of the system, instead of several partial reliability indices. Several approaches have been presented for combining the partial components of a system. In this paper, SCM that is one of the most popular ones was utilized. Conducting the system reliability analysis through SCM involves the calculation of reliability indices and the correlation matrix of all failure modes.

$$S_d = \frac{R_s}{FS_S} \tag{22}$$

$$M_d = \frac{R_M}{FS_M} \tag{23}$$

Table 12 Target reliability indices (Engineers UACo 1997)

Performance level	β	P_f
High	5.0	2.871E-7
Good	4.0	3.169E-5
Above average	3.0	1.350E-3
Below average	2.5	6.210E-3
Poor	2.0	2.275E-2
Unsatisfactory	1.5	6.681E-2
Hazardous	1.0	1.587E-1

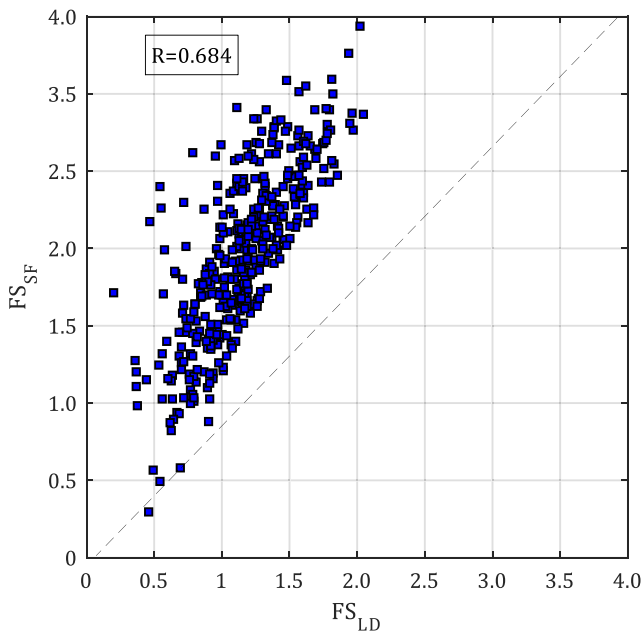


Fig. 37 Determination of correlation between FS_{SF} and FS_{LD} in the saturated state

$$\rho_{sat} = \begin{bmatrix} FS_{BM} & FS_{SF} & FS_{LD} & FS_G \\ 1 & 0.867 & 0.731 & 0.799 & FS_{BM} \\ & 1 & 0.590 & 0.849 & FS_{SF} \\ & & 1 & 0.464 & FS_{LD} \\ sym & & & 1 & FS_G \end{bmatrix} \quad (24)$$

$$\rho_{unsat} = \begin{bmatrix} FS_{BM} & FS_{SF} & FS_{LD} & FS_G \\ 1 & 0.767 & 0.709 & 0.713 & FS_{BM} \\ & 1 & 0.684 & 0.832 & FS_{SF} \\ & & 1 & 0.425 & FS_{LD} \\ sym & & & 1 & FS_G \end{bmatrix} \quad (25)$$

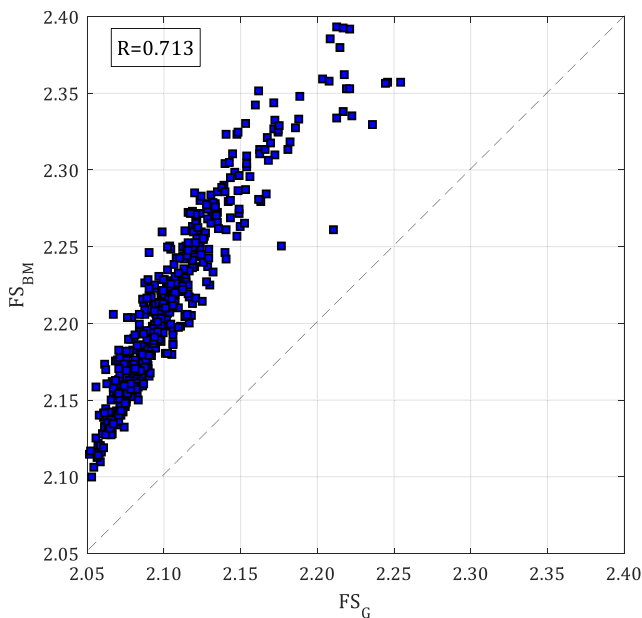


Fig. 38 Determination of correlation between FS_{BM} and FS_G in the unsaturated state

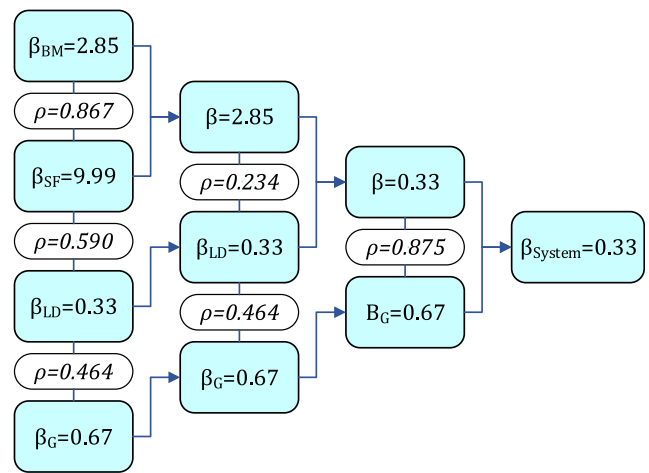


Fig. 39 The procedure for determining the soldier-piled excavation system reliability index in the saturated state

To estimate the correlation matrix, which indicates how the failure modes depend on each other, the correlation between each failure mode with other failure modes must be determined. For this purpose, the correlation between FSs of two failure modes was used to estimate the correlation coefficient (Johari et al. 2020). This procedure was utilized for all components and the results were collected to the correlation matrix, Eqs. (24) and (25) for the saturated and unsaturated state, respectively. Two typical samples for determining the correlation between different failure modes in saturated and unsaturated states are shown in Figs. 37 and 38, respectively. Moreover, the procedure of determining the overall reliability of the soldier-piled excavation system is illustrated in Figs. 39 and 40, for the saturated and unsaturated state, respectively. It can be seen that by taking the unsaturated state into account, the overall reliability index improved from 0.33 to 2.95, or in other words, the performance level shifted from hazardous to above (Engineers UACo 1997).

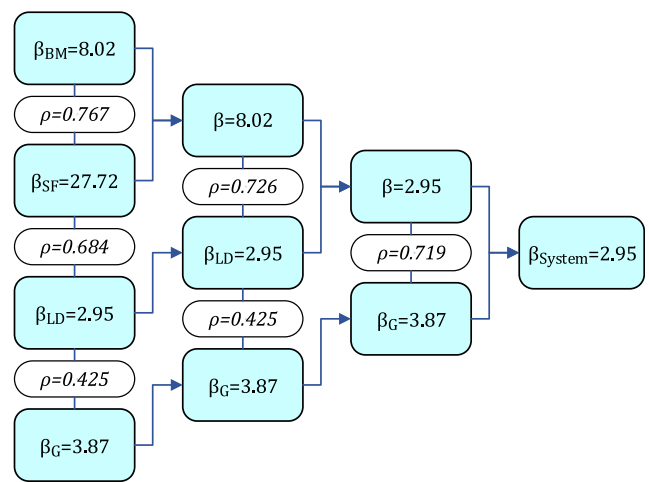


Fig. 40 The procedure for determining the soldier-piled excavation system reliability index in the unsaturated state

Conclusions

Most of retaining systems problems such as soldier-piled excavation generally consist of multiple failure modes and are located in unsaturated areas. Furthermore, complex geological deposition, post-deposition processes, and limited site investigation data can result in the spatial variability of soil properties.

However, addressing these issues simultaneously has not been paid enough attention to, and only some aspect of the object is investigated in the literature. In the current study, a system reliability analysis of a soldier-piled unsaturated excavation was examined. For this purpose, a real site with two boreholes of 20 m depth was considered and the soil parameters were estimated via field and laboratory tests. To simulate the unsaturated soil condition, the SWRC was determined for different depths using a physico-empirical method. Knowing the ω_c and SWRC for each depth, the suction was obtained and implemented in analysis. The analysis was carried out deterministically using the elasto-plastic finite element-based program coded in MATLAB. Then, the stochastic analysis was performed using RFEM by the implementation of a random field with normal distribution to take into account the inherent uncertainty associated with soil parameters (i.e., cohesion, friction angle, and unit weight). In this way, in the unsaturated state, ω_c was considered as a stochastic parameter and consequently, suction for each element was calculated using related SWRC. The reliability indices of all individual failure modes (i.e., global, lateral displacement, shear force, and bending moment) were extracted. Finally, the soldier-piled excavation was modeled as a four-component series system (i.e., global, lateral displacement, shear force, and bending moment) and the SCM was used as an efficient numerical procedure to obtain system reliability index from the reliability indices of individual failure modes. The most important observations can be summarized as follows.

From PDF of FS with respect to all failure modes, it was illustrated that considering the unsaturated state will increase the mean value of FS with respect to lateral displacement, shear force, bending moment, and global stability by 36.2, 45.3, 44.1, and 43.4%, respectively. Also, it was found that implementing suction into model decreases the standard deviations of FS with respect to lateral displacement, shear force, bending moment, and global stability by 35.1, 29.1, 12.5, and 29.3%, respectively, which can be counted as a goal of reliability analysis.

Comparing the COV of failure modes revealed that the impact of the soil properties' uncertainty on global stability is high in comparison to others, while shear force failure mode is less affected than others.

The results highlighted the great significance of the suction in improving reliability indices of failure modes, which changes the stability condition performance level.

The correlation matrix, which indicates how the failure modes depend on each other, showed that the failure mode with respect to shear force and bending moment are strongly correlated with each other in both saturated and unsaturated state.

Results of system reliability analysis indicated that neglecting system reliability analysis lead to overestimated reliability indices. Besides, the results revealed that global failure is the primary mechanism compared to other failure modes, and therefore it determines the probability of the overall failure to a large extent.

However, the proposed method evaluates the stochastic behavior of soldier-piled excavation in an unsaturated state, but rainfall effects such as variation of pore water pressure, soil stiffness, and hydraulic parameters were not considered. Hence, further researches are required to study the application of the proposed method in soldier-piled excavation subject to rainfall effects.

CRediT authorship contribution statement Ali Johari: Conceptualization, methodology, writing—review and editing, supervision, formal analysis, validation.

Alireza Kalantari: Software, methodology, writing—original draft, investigation, validation.

Data availability Some or all data, models, or code that support the findings of this study are available from the corresponding author upon reasonable request.

Appendix

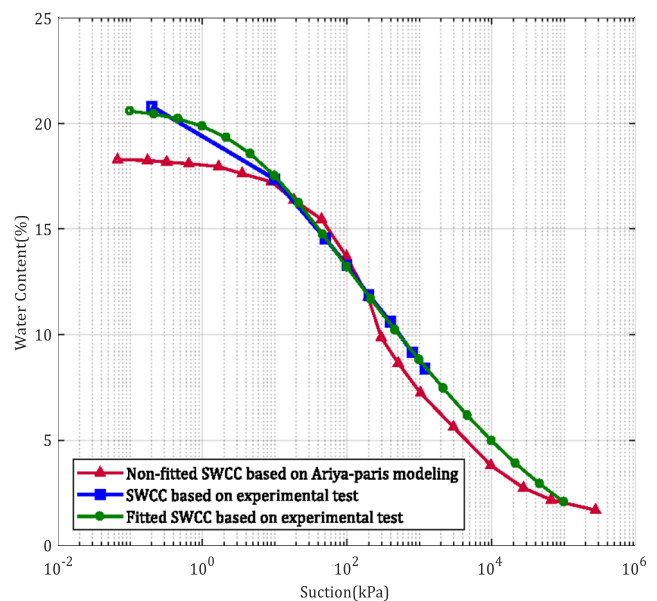


Fig. 41 Determination of fitting parameters “ a ” and “ b ” for sample no. 1 ($a = -2.60$, $b = 1.65$)

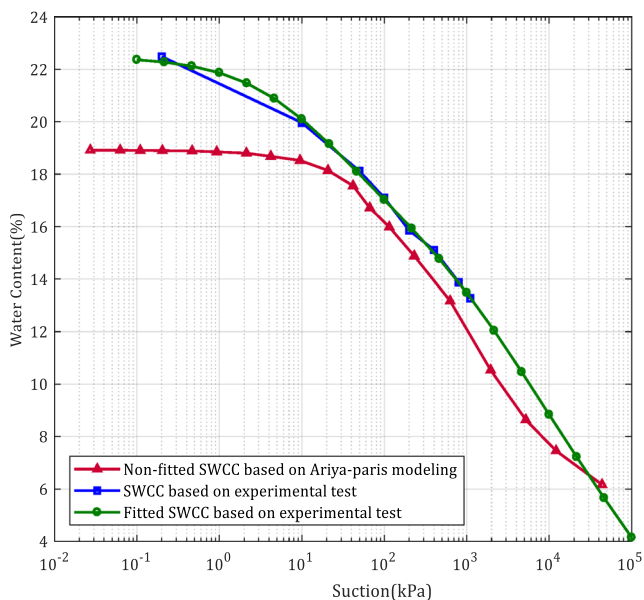


Fig. 42 Determination of fitting parameters “ a ” and “ b ” for sample no. 13 ($a = -2.75$, $b = 1.50$)

Table 13 Best values of “ a ” and “ b ” parameters for soil samples from the city of Shiraz

Sample no.	Classification	LL (%)	PI (%)	ω_c (%)	a	b
1	ML	20	5	14.0	-2.60	1.65
2	CL	28	7	20.0	-2.60	1.50
3	CL	28	11	18.0	-2.60	1.50
4	ML	19	2	15.0	-2.50	1.50
5	CL-ML	27	7	21.5	-2.60	1.45
6	ML	21	3	15.2	-2.60	1.45
7	ML	24	4	15.2	-2.90	1.70
8	ML	21	5	12.5	-2.90	1.70
9	ML	22	3	15.0	-2.50	1.50
10	CL	32	12	18.5	-2.50	1.40
11	CL-ML	24	6	17.0	-2.50	1.50
12	CL	28	9	18.0	-3.00	1.40
13	CL	26	7	17.0	-2.75	1.50
14	CL	23	6	15.5	-2.95	1.60

References

Ahmed A (2012) Simplified and advanced approaches for the probabilistic analysis of shallow foundations. PhD thesis, University of Nantes
 Arya LM, Paris JF (1981) A physicoempirical model to predict the soil moisture characteristic from particle-size distribution and bulk density data. 1 Soil Sci Soc Am J 45:1023–1030
 Arya LM, Leij FJ, van Genuchten MT, Shouse PJ (1999) Scaling parameter to predict the soil water characteristic from particle-size distribution data. Soil Sci Soc Am J 63:510–519
 Assouline S, Tessier D, Bruand A (1998) A conceptual model of the soil water retention curve. Water Resour Res 34:223–231

Baecher GB, Christian JT (2005) Reliability and statistics in geotechnical engineering. Wiley
 Bishop AW (1959) The principle of effective stress. Teknisk ukeblad 39: 859–863
 Brinkgreve R, Kumarswamy S, Swolfs W, Waterman D, Chesaru A, Bonnier P (2014) Plaxis 2014 PLAXIS bv, the Netherlands
 Burland J, Potts D, Walsh N (1981) The overall stability of free and propped embedded cantilever retaining walls. Ground Eng:14
 Cami B, Javankhosdel S, Phoon K-K, Ching JJA-AJoR, Uncertainty in Engineering Systems PACE (2020) Scale of fluctuation for spatially varying soils: estimation methods and values 6:03120002
 Cherubini C (2000) Reliability evaluation of shallow foundation bearing capacity on $c' \phi'$ soils. Can Geotech J 37:264–269
 Engineers UACo (1997) Engineering and design: introduction to probability and reliability methods for use in geotechnical engineering Engineer Technical Letter
 Fenton GA, Griffiths D (2003) Bearing-capacity prediction of spatially random $c \phi$ soils. Can Geotech J 40:54–65
 Fredlund DG, Xing A (1994) Equations for the soil-water characteristic curve. Can Geotech J 31:521–532
 Fredlund MD, Fredlund D, Wilson GW (2000) An equation to represent grain-size distribution. Can Geotech J 37:817–827
 Fredlund MD, Wilson GW, Fredlund DG (2002) Use of the grain-size distribution for estimation of the soil-water characteristic curve. Can Geotech J 39:1103–1117
 Gao G-H, Li D-Q, Cao Z-J, Wang Y, Zhang L (2019) Full probabilistic design of earth retaining structures using generalized subset simulation. Comput Geotech 112:159–172
 Garven E (2006) Evaluation of empirical procedures for predicting the shear strength of unsaturated soils. In: Proceedings of the Fourth International Conference on Unsaturated Soils 2006, pp 2570–2592
 Genz A, Bretz F (2002) Comparison of methods for the computation of multivariate t probabilities. J Comput Graph Stat 11:950–971
 Griffiths D, Fenton GA (1993) Seepage beneath water retaining structures founded on spatially random soil. Geotechnique 43:577–587
 Griffiths D, Fenton GA (2004) Probabilistic slope stability analysis by finite elements. J Geotech Geoenviron 130:507–518
 GuhaRay A, Baidya DK (2015) Reliability-based analysis of cantilever sheet pile walls backfilled with different soil types using the finite-element approach. Int J Geomech 15:06015001
 Huang H, Xiao L, Zhang D, Zhang J (2017) Influence of spatial variability of soil Young's modulus on tunnel convergence in soft soils. Eng Geol 228:357–370
 Jaksa MB (2013) Assessing soil correlation distances and fractal behavior. In: Foundation Engineering in the Face of Uncertainty: Honoring Fred H. Kulhawy. pp 405–420
 Johari A, Gholampour A (2018) A practical approach for reliability analysis of unsaturated slope by conditional random finite element method. Comput Geotech 102:79–91
 Johari A, Golkarfard H (2018) Reliability analysis of unsaturated soil sites based on fundamental period throughout Shiraz, Iran. Soil Dyn Earthq Eng 115:183–197
 Johari A, Lari AM (2017) System probabilistic model of rock slope stability considering correlated failure modes. Comput Geotech 81:26–38
 Johari A, Mousavi S (2019) An analytical probabilistic analysis of slopes based on limit equilibrium methods. Bull Eng Geol Environ 78: 4333–4347
 Johari A, Habibagahi G, Ghahramani A (2011) Prediction of SWCC using artificial intelligent systems: a comparative study. Sci Iranica 18:1002–1008
 Johari A, Hajivand AK, Binesh S (2020) System reliability analysis of soil nail wall using random finite element method. Bull Eng Geol Environ:1–22

- Kang W-H, Song J (2010) Evaluation of multivariate normal integrals for general systems by sequential compounding. *Struct Saf* 32:35–41
- Li C-C, Der Kiureghian A (1993) Optimal discretization of random fields. *J Eng Mech* 119:1136–1154
- Li R, Yu Y, Deng L, Li G (2006) Stability analysis of unsaturated soil slope by 3-D strength reduction FEM. In: *Proceedings of the Sessions of GeoShanghai: Advances in Unsaturated Soil, Seepage, and Environmental Geotechnics*, pp 62–69
- Liu H, Low BK (2017) System reliability analysis of tunnels reinforced by rockbolts. *Tunn Undergr Space Technol* 65:155–166
- Luo Z, Das B (2016) System probabilistic serviceability assessment of braced excavations in clays. *Int J Geotech Eng* 10:135–144
- Luo Z, Li Y, Zhou S, Di H (2018) Effects of vertical spatial variability on supported excavations in sands considering multiple geotechnical and structural failure modes. *Comput Geotech* 95:16–29
- Metya S, Mukhopadhyay T, Adhikari S, Bhattacharya G (2017) System reliability analysis of soil slopes with general slip surfaces using multivariate adaptive regression splines. *Comput Geotech* 87:212–228
- Nguyen TS, Likitlersuang S (2019) Reliability analysis of unsaturated soil slope stability under infiltration considering hydraulic and shear strength parameters. *78:5727–5743*
- Nguyen TS, Likitlersuang S, Ohtsu H, Kitaoka T (2017) Influence of the spatial variability of shear strength parameters on rainfall induced landslides: a case study of sandstone slope in Japan. *10:369*
- Nguyen TS, Likitlersuang S, Jotisankasa A (2019) Influence of the spatial variability of the root cohesion on a slope-scale stability model: a case study of residual soil slope in Thailand. *Bull Eng Geol Environ* 78:3337–3351
- Pandey MD, Sarkar A (2002) Comparison of a simple approximation for multinormal integration with an importance sampling-based simulation method. *Probabilistic Eng Mech* 17:215–218
- Parhizkar A, Ataei M, Moarefvand P, Rasouli V (2012) A probabilistic model to improve reconciliation of estimated and actual grade in open-pit mining. *Arab J Geosci* 5:1279–1288
- Phoon K-K, Kulhawy FH (1999) Evaluation of geotechnical property variability. *Can Geotech J* 36:625–639. <https://doi.org/10.1139/t99-039>
- Rahman MM, Nguyen HBK (2012) *Applications of random finite element method in bearing capacity problems*. Xpert Publishing Services
- Sahoo JP, Ganesh R (2018) Active earth pressure on retaining walls with unsaturated soil backfill. In *Cham. Ground improvement and earth structures*. Springer International Publishing, pp 1–19
- Sert S, Luo Z, Xiao J, Gong W, Juang CH (2016) Probabilistic analysis of responses of cantilever wall-supported excavations in sands considering vertical spatial variability. *Comput Geotech* 75:182–191
- Shwan B (2016) Analysis of passive earth thrust in an unsaturated sandy soil using discontinuity layout optimization. *E3S Web Conf* 9: 08018
- Smith IM, Griffiths DV, Margetts L (2013) *Programming the finite element method*. Wiley
- Tang Y-g (2011) Probability-based method using RFEM for predicting wall deflection caused by excavation. *J Zhejiang Univ Sci A* 12: 737–746
- Tekinsoy MA, Kayadelen C, Keskin MS, Söylemez M (2004) An equation for predicting shear strength envelope with respect to matric suction. *Comput Geotech* 31:589–593
- Vahedifard F, Leshchinsky BA, Mortezaei K, Lu N (2015) Active earth pressures for unsaturated retaining structures. *J Geotech Geoenviron* 141:04015048
- Vanapalli S, Fredlund D, Pufahl D, Clifton A (1996) Model for the prediction of shear strength with respect to soil suction. *Can Geotech J* 33:379–392
- Vanmarcke E (1983) *Random fields: analysis and synthesis*, 1983. MIT Press, Cambridge
- Vo T, Russell AR (2014) Slip line theory applied to a retaining wall–unsaturated soil interaction problem. *Comput Geotech* 55:416–428
- Vo T, Russell AR (2016) Interaction between retaining walls and unsaturated soils in experiments and using slip line theory. *J Eng Mech* 143:04016120
- Wang Y (2013) MCS-based probabilistic design of embedded sheet pile walls. *Georisk* 7:151–162
- Wu XZ (2013) Trivariate analysis of soil ranking-correlated characteristics and its application to probabilistic stability assessments in geotechnical engineering problems. *Soils Found* 53:540–556
- Zevgolis IE, Bourdeau PL (2010) Probabilistic analysis of retaining walls. *Comput Geotech* 37:359–373
- Zevgolis IE, Daffas ZA (2018) System reliability assessment of soil nail walls. *Comput Geotech* 98:232–242
- Zhang L (2009) Nonlinear analysis of laterally loaded rigid piles in cohesionless soil. *Comput Geotech* 36:718–724
- Zhang W, Goh AT, Zhang Y (2015) Probabilistic assessment of serviceability limit state of diaphragm walls for braced excavation in clays ASCE-ASME. *J Risk Uncertain Eng Syst A Civ Eng* 1:06015001